Theoretical and Experimental Studies of a Charge-Transfer Mechanism for Biomimetic Oxygenations of Phenol and Indol Derivatives

Yasunori Yoshioka,# Syusuke Yamanaka, Satoru Yamada, Takashi Kawakami, Masamichi Nishino, Kizashi Yamaguchi,* and Akira Nishinaga†

Department of Chemistry, Faculty of Science, Osaka University, Toyonaka, Osaka 560

†Department of Applied Chemistry, Osaka Institute of Technology, Ohmiya 5, Asahi-ku, Osaka 535

(Received September 11, 1995)

The structures and stabilities of organodioxide anions, charge-transfer (CT) complexes between carbanions and molecular oxygen, and related solvated clusters were investigated using ab initio and semiempirical MO plus intermolecular CT theories. The computational results, together with experimental evidence, have revealed the characteristics of potential curves, indicating that the nonradical mechanism via CT complexes is operative for base-catalyzed dioxygenation reactions of phenol and indole derivatives. The following conclusions were drawn from the present calculations: (1) The reactions of carbanion with triplet molecular oxygen proceed through a one-electron transfer (ET) mechanism from carbanion to $^3O_2$. (2) The base-promoted phenol monoanion reacts with molecular oxygen via two different mechanism: one is the CT mechanism, where the triplet CT complex is formed and a spin inversion from a triplet CT complex to a singlet CT one occurs in aprotic solvents; the other involves the one ET mechanism assisted by hydrogen bonding in a protic solvent. (3) The one ET does not occur for the free monoanions of the indole derivatives; rather these species are readily oxygenated by organo-cobalt catalysts. (4) For the flavin derivatives, the CT mechanism is applicable in an aprotic solution, while both the CT and one ET mechanisms are conceivable in aqueous solution. The implications of these results to biological dioxygenations by metallo-dioxygenases are discussed in relation to biomimetic oxygenations of phenol and indole derivatives.

The incorporation of molecular oxygen into organic compounds is one of the most important processes not only in the metabolism of living things, but also in organic syntheses.[1—8] In biological oxygenations catalyzed dioxygenases, the reactions proceed in a highly regioselective manner.[3,9] On the other hand, the dioxygenation takes place exothermically when a carbon radical is involved in the process. The oxygenations of this type usually include a radical chain process, the control of which is quite difficult for selective oxygenations, giving rise to crucial by-products which seem not to be involved in biological dioxygenations. Therefore, clarifying the mechanism for highly selective dioxygenations is quite interesting and important for understanding the biological oxygenations and the development for new techniques in organic syntheses as well. Metallodioxygenations contain in their catalytic reaction center iron or copper ion, whose complexes often interact with molecular oxygen to function as oxygen carriers.[10] On this ground, dioxygen activation by these metal ions has been suggested for biological dioxygenations.[2] However, recent spectroscopic studies of 1,2-dioxygenase and protocatechate 3,4-dioxygenase reactions have revealed that the iron(III) state in the reaction center of these enzymes is retained during the course of the reactions without a reduction to the iron(II) state by substrates;[11,12] namely, it seems to work like a base to accept a proton from the species, although the involvement of an electron transfer, leading to an intermediary formation of a substrate radical and a superoxoiron species, has recently been discussed.[13,14] Recent EPR studies on the oxygenation of some model catecholato–iron(III) complexes, on the other hand, have shown that an iron(III)-monodentate dianionic catecholato complex intermediate is the O_2 reactive species, into which dioxygen is incorporated in a nonradical manner.[15] This implies that the role of the reaction center of the enzymes is not to activate dioxygen, but to activate substrates so as to produce the corresponding substrate anions into which molecular dioxygen is incorporated.[16] A similar activation process has been experimentally proposed for the dioxygenations of phenol,[17] indole,[18] and flavonols[19] derivatives promoted by a base and/or cobalt-Schiff base complexes as models for these dioxygenation reactions.

The base-promoted oxygenation of organic compounds, resulting in dioxygen incorporation into a carbanion, was intensively investigated by Russel et al.[20] and Walling et al.[21] They proposed the so-called autoxidation mechanism, which involves substrate radicals produced by a one-electron-transfer (ET) form carbanions to dioxygen. On the contrary, Nishinaga et al.[17—19] have shown that base-promoted dioxygenations of *t*-butylphenoles (**I**) in aprotic me-

Takasago Laboratories, Kaneka Corporation, Miyamaemachi, Takasago-cho, Takasago, Hyogo 676.

dia do not involve phenoxyl radicals, suggesting that the radical-chain mechanism is not operative in their dioxygenations. Thus, the experiments show that molecular complexes formed by interactions between anionic species and triplet molecular oxygen play important roles in the base-catalyzed oxygenations of various substrates.

We previously examined CT complex formations between extremely electron-rich olefins and triplet molecular oxygen on the basis of intermolecular configuration interaction (ICI) theory.[22] It was shown that the CT followed by the spin inversion (CTSI) mechanism could be operative for the oxygenations of these species[22] in accord with the findings by Turro et al.[23] The experimental findings of Nishinaga et al.[17] together with our previous theoretical calculations,[24] indicate the necessity to distinguish between free radical autoxidation and the charge-transfer (CT) complex mechanism for the base-promoted oxygenations of organic molecules (vide supra), although no systematic theoretical investigation has yet been made in this area. In fact, judging from previous MO-theoretical calculations of 1,3-dipolar[24e] and 1, 4-dipolar species,[24f] the electronic properties of the intermediates in the oxygenation reactions of anionic species (D^-) could be variables within the discrete extremes: namely, the closed-shell (nonradical) organodioxide anion **1** and a complete one electron-transfer biradical (ET BR) (**2**). In the latter extreme, free radicals (D·) are often released out from the solvent cage.[20,21]

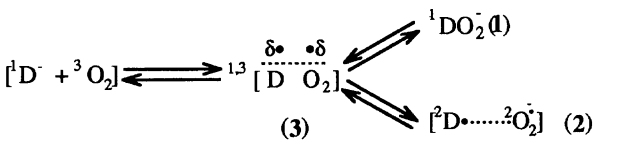

(1)

Intermediates **1**, **2**, and the CT complexes (**3**) in Eq. 1 belong to the nonradical (region I), biradical (region III) and intermediate (region II) cases from the previously presented MO-theoretical view point.[24e,24f]

As shown previously,[24] the restricted Hartree–Fock (RHF) molecular orbital (MO) method can be applied to elucidate the electronic structures of organodioxide anion **1**, carbanions, peroxide anions etc., which are essentially regarded as being closed-shell species. However, the RHF MO method does not work well in the case of the ET biradical species (**2**) generated during the course of the oxygenation reactions of organic compounds. On the other hand, the unrestricted HF (UHF) MO method, which allows the different orbitals for different spins (DODS),[24] was successfully applied to examine the an ET BR character for such unstable species. The state correlation diagrams for organic reactions via ET BR intermediate were also calculated by the complete active space (CAS) configuration interaction (CI) method using the UHF natural orbitals (UNO): UNO CAS CI.[22d] The UNO CAS CI calculations[24d] supported the qualitative DODS MO-theoretical descriptions of the ET BR species formed in organic reactions.[24a,24b,24c]

In this paper we describe both ab initio and semiempirical MO-theoretical calculations[24] of organodioxide anions which could be formed in the base-catalyzed oxygenations of the parent phenol (**II**), indole (**III**), and arylalkanes (**IV**). The electron affinity of molecular oxygen were first examined in relation to solvations of the superoxide anion radical. Possible biradical (BR) forms for molecular complexes between free radicals and superoxide were also elucidated on the basis of these calculations. The potential curves for the BR states of some typical systems are depicted in both cases with and without hydrogen-bonding stabilization or stabilization by the genen cation. The MO-theoretical results were further used to construct the intermolecular CI (ICI) models for the peroxo complexes of substituted phenols, catechols, and indoles, which are known to be substrates for dioxygenation reactions catalyzed by dioxygenases, such as pyrocatechase and tryptophan 2,3-dioxygenase.[3,8] The ET BR characters for these organodioxide anions were estimated on the basis of these ICI models using the calculated ionization potentials and oxidation potentials of the substrates. The implications of these theoretical results concerning oxygenation reactions of phenol, catechol, indole, and flavin derivatives are discussed in relation to the various experimental results available in this area.

MO-Theoretical Studies of a One Electron-Transfer (ET) Mechanism

1. Electron Affinity of Molecular Oxygen. The simplist one-electron-transfer (ET) reaction of molecular oxygen is its electron capture.[25] The electron affinity (E_A) of the ground-state oxygen ($^3O_2$) was calculated by the ab initio unrestricted HF (UHF) MO method.

$$^3O_2 + e \longrightarrow {}^2O_2^{-\cdot} \qquad (2)$$

Figure 1 illustrates the calculated potential curves of $^3O_2$ and the superoxide anion. It was found that the equilibrium O–O bond lengths of these species are 1.21 and 1.29 (Å), respectively, using the 6-31 G* basis set (BS); they are 1.23 and 1.36 (Å), respectively, using the 4-31G+diffuse (exponent is 0.094) BS. The UHF calculation using the 6-31G* BS reproduces the bond lengths of molecular oxygen and the superoxide anion. However, it gives a negative electron affinity ($E_A = -1.39$ eV) for triplet molecular oxygen. On the other hand, the E_A value was calculated to be essentially zero using the 4-31G+diffuse BS. Since the observed E_A value of triplet molecular oxygenic 0.43 eV[26,27] the latter BS is rather appropriate for the present purpose. Hereafter, the (4-31G+diffuse) BS is referred to as BSI.

Since a Hartree–Fock treatment is insufficient for computing the electron affinity, post Hartree–Fock calculations of $^3O_2$ and O_2^- were also carried out using the 6-31G*+diffuse (exponent is 0.094) BS. The equilibrium O–O bond lengths of $^3O_2$ and O_2^- were calculated to be 1.24 and 1.39 Å, respectively, at the UHF Moller–Plesset fourth-order (UMP4) level, and the resulting electron affinity (E_A) of molecular oxygen was 0.13 eV. On the other hand, the corresponding O–O lengths were 1.231 and 1.375 Å based on the UHF

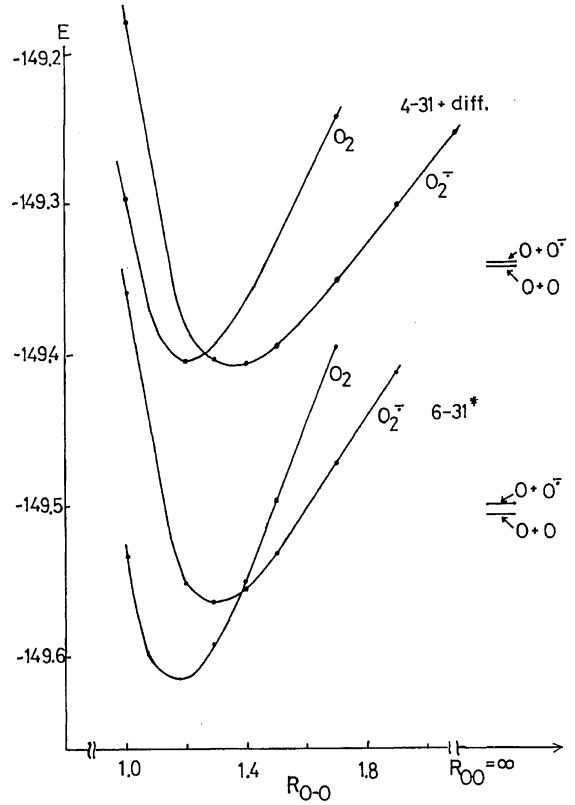

Fig. 1. The potential curves of triplet molecular oxygen and superoxide anion calculated by the ab initio UHF method.

coupled-cluster (UCC) single (S), double (D), and triplet (T) excitation (SD(T)) method; the E_A-value was 0.14 eV, still smaller than the experimental value (0.43 eV).[26,27] Thus, pure nonempirical calculations of the relative energies for oxygen-containing compounds are hard task even at the UCC SD-(T)/6-31G*+diffuse BS. Therefore, we perform rather qualitative ab initio MO calculations using BSI, together with semiempirical INDO calculations. The BS plus correlation corrections for potential curves obtained by these calculations were conducted so as to reproduce various available experimental results.[17—19] For this purpose, the experimental ionization potentials and oxidation potentials were utilized to estimate the CT excitation energies, as shown below.

The electron affinity of triplet molecular oxygen increases in a polar solution because its reduced form, superoxide anion, is greatly stabilized by solvation.[25,28—30] Stabilization of the superoxide anion by the hydrogen bonding is particularly important, since it accelerates the electron transfer from donor to triplet oxygen. The clustering energy of one water to superoxide anion was calculated to be 19.2 kcal mol^{-1} by the UHF (BSI) geometry optimization technique. The calculated value was closed to the observed one (18.4 kcal mol^{-1}).[28] On the other hand, it was 21.3 kcal mol^{-1} based on the 4-31 G basis set, which is referred to as BSII. Assuming the optimized hydrogen-bonding distance (R_{O-H}=1.80 Å), the clusterings of two and four water molecules to superoxide (Fig. 2) were examined by the UHF (BSII) method. The calculated clustering energy of four water molecules is 64.2 kcal mol^{-1}, which is about 2/3 of that for the solvation energy of superoxide in aqueous solution, in which the two water molecules coordinate each oxygen site, namely $(H_2O)_2$ O---O $(H_2O)_2$.[30] The clustering energy calculated for this symmetric structure could be over 70 kcal mol^{-1}.[30] Because of the large solvation energy, the electron affinity of triplet molecular oxygen is comparable to that of 9,10-dicyanoanthracene (DCA) in aqueous solution, although DCA is a far stronger electron acceptor in the gas phase.[31]

$$^2O_2^{-\cdot} + n(H_2O) \longrightarrow O_2^{-\cdot}(H_2O)_n \quad (4) \qquad (3)$$

The hydrogen-bonding complex between the superoxide and ammonia (R_{O-H}=1.80 Å) was examined as a model of the hydrogen-bonding stabilization of superoxide by the amino acid residue. The clustering energies of one and two ammonia molecules are 13.1 and 24.5 kcal mol^{-1}, respectively, based on the UHF (BSII) method. These values correspond to about 70% of the clustering energies of water molecules.[25]

$$^2O_2^{-\cdot} + n(NH_3) \longrightarrow {}^2O_2^{-\cdot}(NH_3)_n \quad (5) \qquad (4)$$

The stabilization of superoxide by counter cations, such as lithium and potassium cations, were also examined using the UHF method with (MINI+diffuse) (BSIII) and (MIDI+diffuse) (BSIV) basis sets (BS) by Tatewaki and Hujinaga, and Hay.[32] Figure 3 illustrates the potential curves for the KO_2 system. From Fig. 3, electron transfer occurs from

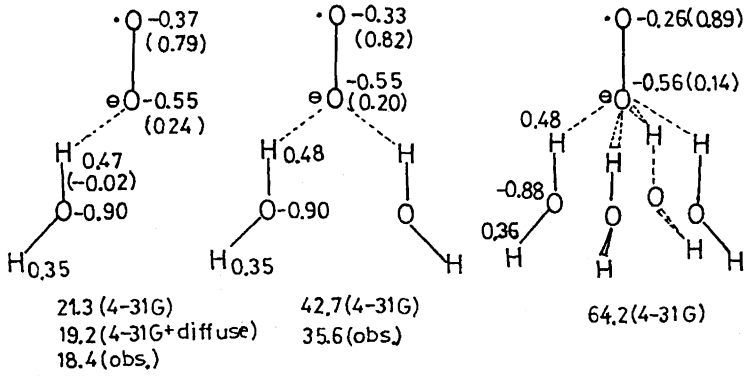

Fig. 2. The clustering energy (kcal mol^{-1}), net charge and spin densities (in parentheses) for the clusters constructed of superoxide anion and water molecules.

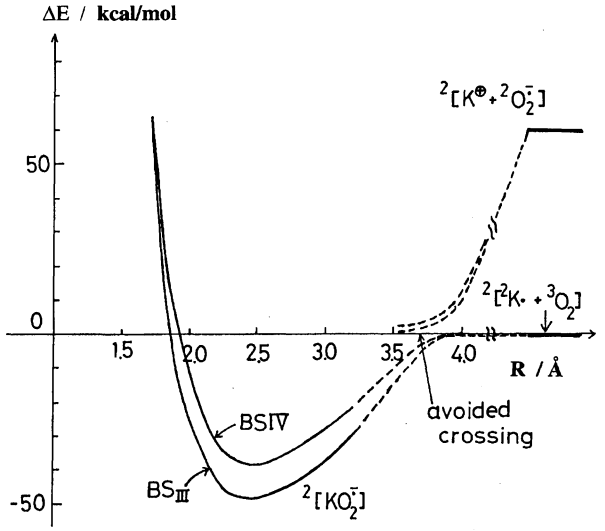

Fig. 3. The potential curves for the potassium plus molecular oxygen by the UHF/BSIII and BSIV (see text) methods.

the potassium atom to molecular oxygen at an intermediary stage, giving the charge-transfer complex **6**:

$$^3O_2 + M \longrightarrow {}^2O_2^{-\bullet}M^+ \quad (\mathbf{6}) \qquad (5)$$

Although stabilization energies (ΔH) were sensitive to the basis sets, the calculated equilibrium distances (R) were almost constant. The net electron transfer was calculated to be almost 1.0 for the system. On the other hand, it was 0.73 for the LiO_2 system because of the smaller ionic radius of the lithium cation and the covalent bonding character between Li–O atoms. Several groups[10a,33] already calculated the net electron transfers from ligands to molecular oxygen in the transition metal–oxygen complexes to elucidate the oxygen activations by transition-metal complexes. The results are summarized in Table 1, which shows that the net electron transfer from the transition-metal complexes to molecular oxygen are 0.0—0.8. The ET BR characters (or superoxide character in this case) for the complexes are variable within the extreme formal pictures, one ET **7a** and no ET **7b** structures, depending on the kind of transition metal ions (M(n)) and ligands (Lm). The situations are similar in the case of the BR characters of tricentric bisdesmiphiles and 1,4-dipoles comprising singlet oxygen and enol ethers, which were previously investigated.[24] In fact, these labile electronic structures are common characteristics appearing in the complex reaction systems under consideration.

$$^3O_2 + M(n)Lm \longrightarrow {}^-OOM(n+1)Lm\ (\mathbf{7a})\ \text{or}\ OOM(n)Lm\ (\mathbf{7b}) \quad (6)$$

2. One-Electron Transfer (ET) form Carbanions to Molecular Oxygen. The thermal electron-transfer (ET) reaction from carbanion to molecular oxygen has been regarded as being one of the crucial steps in the autoxidation of arylalkanes (**IV**); for example,[8]

$$R_3C^-(\mathbf{IV}) + {}^3O_2 \longrightarrow R_3C^{\bullet}(\mathbf{IV}) + {}^2O_2^{-\bullet} \quad (\mathbf{8}) \qquad (7)$$

As a model of reaction (7), the methanide anion plus molecular oxygen system was examined, as shown in Fig. 4. Since the electron affinity of the methyl radical was calculated to be negative by the UHF/BSI (exponent of diffuse function: $\alpha_c = 0.061$), the present model represents the case in which the electron affinity of the free radical ($R_3C\cdot$) is far less than that of triplet molecular oxygen. Thus, the one electron transfer from a methanide anion to triplet molecular oxygen is exothermic, being considered to be diffusion-controlled. In fact, the ground state of the system was found to be the ET biradical (ET BR) pair in the larger intermolecular region, $R_1 > 3.0$ Å. Therefore, the ET reaction is actually regarded as being the reverse process of a recombination between the methyl radical and the superoxide anion. Figure 5A illustrates the potential curves of the singlet and triplet BR states by the UHF (BSI) method:

$$H_3C\cdot + \cdot O\text{–}O^- \longrightarrow H_3C\text{–}O\text{–}O^- \quad (\mathbf{9a}) \qquad (8)$$

There appears two ET BR states with different spatial symmetries depending on the orientations of the radical lobes, as illustrated in Fig. 6. One (symmetric (S)-state) is referred to as the $\sigma\sigma$-BR, whose singlet component correlates to the organodioxide anion passing through the avoided

Table 1. Net Electron Transfers and Heats of Formation for Metal Oxygen Complexes

System		BS[b]	Net ET	ΔH[c]	Ref.
LiO_2		BSV[a]	−0.73	−35	Present
KO_2		BSIII	−0.99	−48	Present
		BSIV	−0.98	−38	Present
	Lm=none	I	−0.44	46	33a
	Lm=H_2O	I	−0.50	34	33a
$CoLmO_2^-$	Lm=CO	I	−0.57	29	33a
(acacen)	Lm=Im	I		25 (−17)[d]	33a
	Lm=CN	I	−0.47	−16	33a
$TiPoO_2$[e]		I	−0.66		33f
$MnPoO_2$		I	−0.45		33f
$Fe(NH_3)PoO_2$		I	0.02		33f
$Co(NH_3)PoO_2$		I	−0.45		33f
$FeImPoO_2$		II	−0.75		33g
		III	−0.08		33g
$FeImPoO_2$		PPP	0.04		33e
$(NH_3)PoO_2$		I	−0.65		33h

a) BSV=6-31 G*+diffuse. b) I: ab-initio, II, III: semiempirical. c) kcal mol^{-1}. d) Observed value (Ref. 9). e) Po=porphyrin.

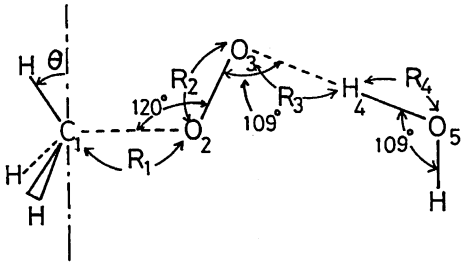

Fig. 4. Approach models of superoxide and superoxide plus water toward methyl radical. R_1 is the intermolecular distance and θ is the deformation angle; $\theta = 19°$ or methyl anion.

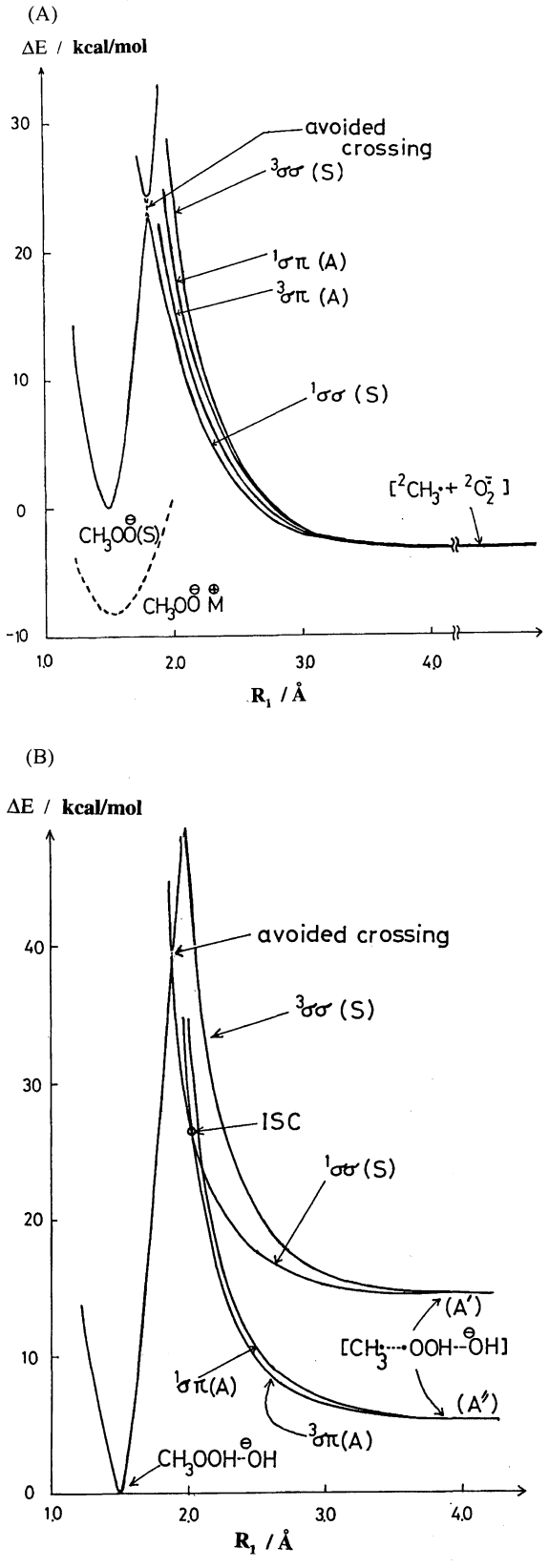

Fig. 5. (A) Potential curves calculated for the recombination process between methyl radical and superoxide anion by UHF (BSI) method. The dotted line indicates the modified curve by the coordination of a gegen metal ion; (B) Potential curves calculated for the recombination process between methyl radical and superoxide plus water by the UHF (BSI) method.

crossing point near to the transition state (TS). The other (antisymmetric (A) state) is the $\sigma\pi$-BR state, which is characterized by a repulsive potential curve. There is a large activation barrier (E_a=24 kcal mol^{-1}) for the recombination process. This implies that the radical chain reactions (Eqs. 10a and 10b) are preferred to the recombination process (Eq. 8) in accord with the Russell mechanism.

$$\sigma\sigma\text{-BR } (\mathbf{10}) \longrightarrow {}^1\text{TS} \longrightarrow CH_3OO^- \ (\mathbf{9a}) \tag{9}$$

$$H_3C\cdot + {}^3O_2 \longrightarrow H_3COO\cdot \ (\mathbf{9b}) \tag{10a}$$

$$H_3COO\cdot + H_3C^- \longrightarrow H_3COO^- + H_3C\cdot \tag{10b}$$

The organodioxide anions in Eq. 9 could be stabilized by metal ions (M^+) in the case of base-catalyzed oxygenations. The stabilization energies of **9a** by M^+ were calculated by the UHF (BSIV) method.[32] The results are summarized in Table 2. From Table 2, it can be seen that alkali metal ions act effectively to stabilize **9a**, indicating that the potential curve in Fig. 5A is modified, as depicted by

$$CH_3^- + {}^3O_2 \xrightarrow{M^+} CH_3OO^-M^+ \tag{11a}$$

$$R^- + {}^3O_2 \xrightarrow{M(n)Lm} R\text{–}OO^-M(n)Lm \tag{11b}$$

by the dotted line. Similar stabilizations by transition metal ions[10a,33] are probably operative in the case of transition-metal catalyzed oxygenations in Eq. 11b.

3. One-Electron Transfer Assisted by a Proton Transfer. A thermal electron-transfer from the methanide anion to triplet molecular oxygen, assisted by hydrogen bonding, was examined as a model for the hydroperoxidation of an anion site of substrate in a protic solvent.[15h,15k,15l,15m,20,21] Water or ammonia is used as a proton source for computational economy, although the coexistence of carbanion and water is unrealistic because of the rapid reaction between them.

$$R_3C^- + {}^3O_2 + HOR \longrightarrow R_3COOH + {}^-OR \tag{12}$$

In order to study the reaction in Eq. 12, cluster [CH_3^-, $^3O_2$, and H_2O] was examined, as illustrated in Fig. 4. The hydrogen-bonding distance between the terminal oxygen (O_3) and

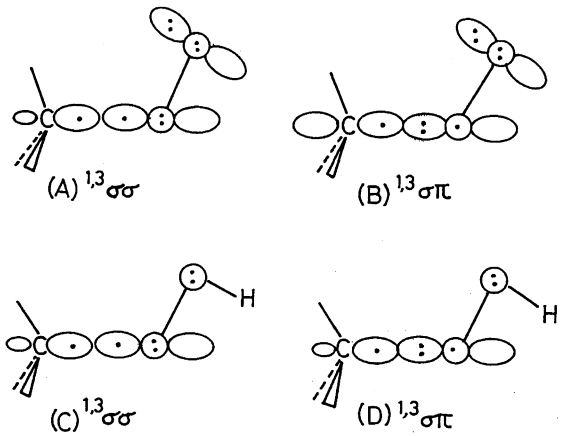

Fig. 6. Orbital configurations for the $\sigma\sigma$ and $\sigma\pi$ ET biradicals of methyl radical plus $O_2\cdot^-$ (A,B) and methyl radical plus $O_2\cdot^-$ (H_2O) (C,D) systems.

Table 2. Relative Energies, Net Charges (ΔP) and Spin Densities (ΔQ) (in Parentheses) for Peroxyanion Intermediates by the UHF Method

Sys.[a]	R	E_{rel}	CT	ΔP (ΔQ)		
				C_1	O_2	O_3
(A) CH_3OO^-	1.5	0.0[b]	0.93	−0.54 (0.0)	−0.17 (0.0)	−0.76 (0.0)
BR $^1\sigma\sigma$	2.0	13.6	0.84	−0.70 (1.20)	−0.24 (−0.60)	−0.60 (−0.30)
$^3\sigma\sigma$	2.0	23.7	0.77	−0.74 (1.31)	−0.39 (0.28)	−0.38 (0.70)
$^1\sigma\pi$	2.0	19.4	0.71	−0.79 (1.27)	−0.29 (−0.45)	−0.42 (−0.55)
$^3\sigma\pi$	2.0	16.2	0.69	−0.80 (1.22)	−0.25 (0.49)	−0.45 (0.56)
$^{1,3}\sigma\sigma$, $^{1,3}\sigma\pi$	6.0	−3.5	1.00	−0.80 (1.35)	−0.50 (0.49)	−0.50 (−0.50)
(B) $CH_3OOH\cdot\cdot^-OH$	1.5	0.0[c]	1.00	−0.51 (0.0)	−0.20 (0.0)	−0.65 (0.0)
BR $^1\sigma\sigma$	2.0	27.0	0.90	−0.68 (1.18)	−0.13 (−0.60)	−0.61 (−0.06)
$^3\sigma\sigma$	2.0	46.3	0.81	−0.73 (1.35)	−0.11 (0.76)	−0.56 (0.17)
$^1\sigma\pi$	2.0	32.6	0.77	−0.75 (1.32)	−0.10 (−0.75)	−0.50 (−0.28)
$^3\sigma\pi$	2.0	29.1	0.75	−0.76 (1.27)	−0.08 (0.75)	−0.51 (0.29)
$^{1,3}\sigma\sigma$	6.0	13.8	1.00	−0.52 (1.35)	−0.25 (−0.87)	−0.59 (−0.10)
$^{1,3}\sigma\pi$	6.0	4.82	1.00	−0.52 (1.35)	−0.29 (−0.76)	−0.53 (−0.26)
(C) $CH_3OO^-Li^+$	1.75	−47.1[d,f]		0.04 (0.0)	−0.35 (0.0)	−0.95 (0.0)
(D) $CH_3OO^-K^+$	2.5	−30.5[e,f]		0.00 (0.0)	−0.31 (0.0)	−0.91 (0.0)

a) BSI for A and B and BSIV for C and D. b) −188.9051 (a.u.). c) −264.8073 (a.u.). d) −195.5218 (a.u.). e) −784.6260 (a.u.). f) The heart of formations in the case of c) and d).

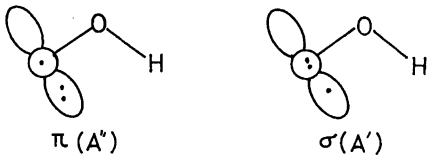

Chart 1.

the proton (H_4) is taken to be very short (R_3=1.21 Å), being responsible for the protonating form of the superoxide, i.e., the hydroperoxyl radical. UHF calculations using the 4-31G+diffuse basis set (BSI) were carried out for changing the intermolecular distance (R_1) in Fig. 4. Figure 5B depicts the calculated potential curve. Table 2 summarizes the calculated total energies, net charges and spin densities for several key intermediates.

The ab initio results show that a complete one-electron transfer (ET) from CH_3^- to $^3O_2$ occurs at R_1>3.0 Å, since the ET BR state is far more stable than the no ET state at the dissociation limit. Thus, the potential curve in Fig. 5B is actually regarded as being that of the radical recombination process:

$$R_3C^{\cdot} + \cdot O\text{–}O\text{–}H\cdots{}^-O\text{–}H \longrightarrow R_3C\text{–}O\text{–}O\text{–}H\cdots{}^-OH \quad (13)$$

The energy difference between $^{1,3}\sigma\sigma$(S) and $^{1,3}\sigma\pi$(A) ET BR states is about 9 kcal mol^{-1} at R=6.0 Å, which corresponds to the energy difference between the A′(σ-radical) and A″ (π-radical) states of the hydroperoxyl radical (Chart 1). Since the A″ state is the ground state of the hydroperoxyl radical, the surface crossings between the $^{1,3}\sigma\sigma$ and $^{1,3}\sigma\pi$ET BR states occur at R=2.3 Å in the C_s symmetry-adapted reaction path, as shown in Fig. 5B. Inter system crossing (ISC) from $^3\sigma\pi$ to $^1\sigma\sigma$ BR is easy because of the curve crossing and nonzero spin-orbit (SO) coupling interaction:

$$\langle {}^1\sigma\sigma|\text{S.O.}|{}^3\sigma\pi\rangle = \langle {}^1\sigma\sigma|\mathbf{s}\cdot\mathbf{1}|{}^3\sigma\pi\rangle = \langle 1|\mathbf{s}|3\rangle\langle\sigma|\mathbf{l}|\pi\rangle \neq 0 \quad (14)$$

A single–triplet spin rotation is induced by the spin operator **s**, whereas σ–π orbital rotation occurs using the angular-momentum operator **1**. The back CT from superoxide plus water to the methyl radical near to the TS region (R_1=2.0 Å) is slightly suppressed by hydrogen-bonding stabilization. The spin densities are essentially localized on the reaction sites, namely C_1 and O_2, for all of the BR intermediates at R_1=2.0 Å, indicating that the TS resembles that of the recombination process between the methyl and hydroperoxyl radicals. However, the calculated activation barrier is not negligible. The radical chain reactions in Eqs. 10a and 10b are therefore feasible even in this case, leading to autoxidations. The product anion was calculated to be more stable by 4.8 kcal mol^{-1} than the ET radical pair, in contrast to the preceding system without the hydrogen-bonding stabilization. This implies that the hydroperoxide is a stable product for the autoxidation process in protic media, in accord with the experimental results.[15h,15k,15l,15m,20,21]

Semiempirical (INDO) calculations were also carried out for the same model in Fig. 4. The results were essentially the same as those of the ab initio calculations. Thus, the INDO method is useful for theoretical studies of relatively larger systems as shown below. From the ab initio and INDO calculations, plausible potential curves for carbanions plus molecular oxygen systems emerged as depicted in Fig. 7A. It was found (1) that the electron-transfer (ET) state is more stable than the no ET state, and (2) that the recombination between the radical pair requires an activation energy.

$$R^- + {}^3O_2 \longrightarrow R\cdot + {}^2O_2^{-\cdot} \quad (15a)$$

$$R\cdot + {}^2O_2^{-\cdot} \longrightarrow ROO^- \quad (15b)$$

$$R\cdot + {}^3O_2 \longrightarrow ROO\cdot \quad (15c)$$

$$ROO\cdot + R^- \longrightarrow ROO^- + R\cdot(\text{chain}) \quad (15d)$$

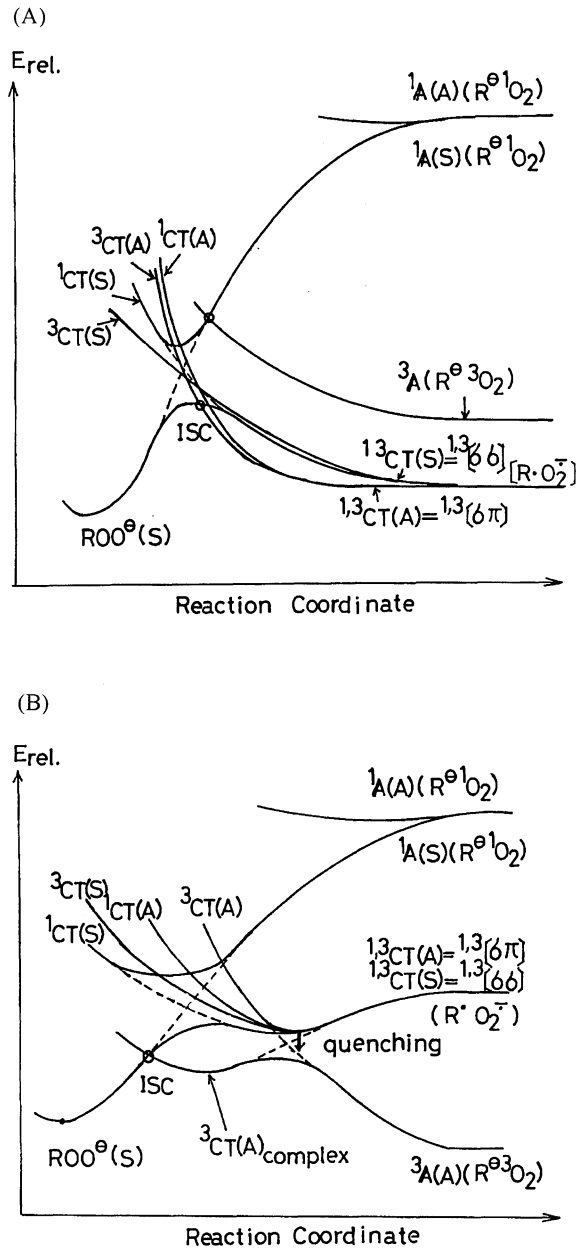

Fig. 7. (A) Proposed potential curves for the carbanions (R^-) plus triplet molecular oxygen systems which undergo the autoxidations in solution phase; (B) Potential curves for the molecular oxygen plus phenoxide monoanion or indole monoanion proposed on the basis of the calculated ΔG values.

$$ROO\cdot + R\cdot \longrightarrow ROOR \qquad (15e)$$

These findings support the radical chain mechanism described by Eqs. 15a—e by Russell.[20] Thus, the model calculations of carbanion systems are consistent with well-established autoxidation mechanisms. However, there are more complex systems in which the CT complexes play essential roles in the case of phenol anions etc., leading to the CT mechanism, as illustrated in Fig. 7B. We return to this problem later.

4. Singlet Oxygen Formations from Organodioxide Anions.

The generations of singlet molecular oxygen in several annihilation processes of the superoxide anion have been extensively investigated.[34] Khan and Kasha have shown singlet oxygen formation in the decomposition reaction of the chlorodioxide anion.[35a] Recently, Adam et al.[35c] suggested $^1O_2$ formation in the base-catalyzed decompositions of hydroperoxides:

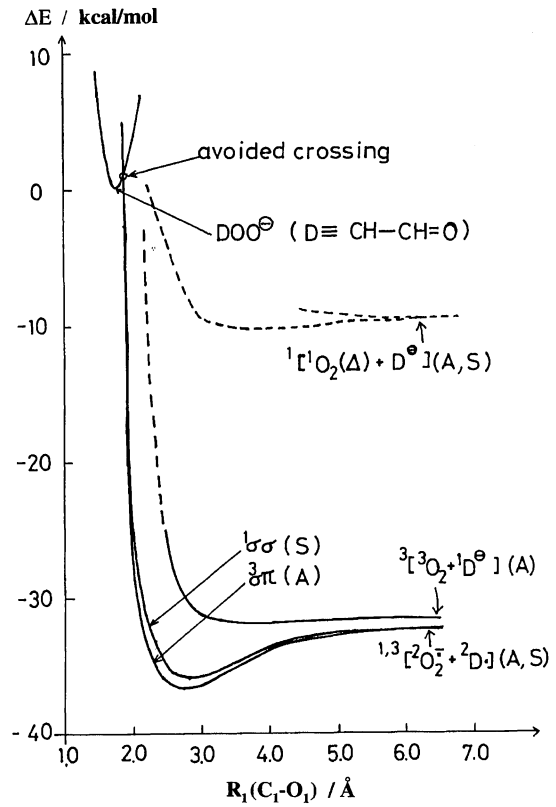

Fig. 8. Potential curves for the decompositions of acylperoxyanion (X=H) by the UHF (BSII) method.

$$O{=}CX{-}COOH \xrightarrow{B^-} O{=}CX{-}\underset{|}{\overset{|}{C}}{-}OO^- \quad (\mathbf{10}) \qquad (16a)$$

$$\mathbf{10} \longrightarrow O{=}CX{-}\underset{|}{\overset{|}{C}}{}^- + {}^1O_2 \qquad (16b)$$

$$\rangle C{=}C{-}\underset{|}{\overset{|}{C}}H + {}^1O_2 \longrightarrow \rangle C{=}C{-}\underset{|}{\overset{|}{C}}{-}OOH \qquad (16c)$$

$$\mathbf{10} \longrightarrow O{=}CX{-}\underset{|}{\overset{|}{C}}{}^- + {}^3O_2 \qquad (16d)$$

If the organodioxide anion (**10**) is less stable over 23 kcal mol^{-1} than its decomposition fragments in Eq. 16d, the $^1O_2$ formation in Eq. 16b is thermodynamically accessible. As a model of these reactions, we examined the decomposition of the most simple organodioxide anion **10b** (X=H). Table 3 summarizes the total energies and net charges for several key intermediates. The heat of decomposition for the species in Eq. 16d was calculated to be -34 kcal mol^{-1}, indicating that $^1O_2$ formation in Eq. 16b is exothermic in the model system, as illustrated in Fig. 8. This implies that $^1O_2$ formation is indeed feasible in the base-catalyzed decomposition of unstable hydroperoxides. However, as recognized

Table 3. Relative Energies, Net Charges (ΔP) and Spin Densities (in Parentheses) for Peroxyenolate

Sys		R	E_{rel}	ΔP (ΔQ)		
				C_1	O_2	O_3
$^-OOCH_2CH{=}O$		1.75	0.0[a]	−0.33 (0.0)	−0.38 (0.0)	−0.56 (0.0)
BR	$^1\sigma\sigma$	2.0	−23.4	−0.29 (−1.06)	−0.37 (0.70)	−0.54 (0.21)
	$^1\sigma\sigma$	3.0	−35.9	−0.26 (−1.20)	−0.50 (0.48)	−0.48 (0.52)
	$^3\sigma\pi$	2.0	−24.9	−0.32 (0.87)	−0.45 (0.37)	−0.30 (0.82)
	$^3\sigma\pi$	3.0	−36.4	−0.26 (1.18)	−0.50 (0.49)	−0.47 (0.53)
	$^1\sigma\sigma$, $^3\sigma\pi$	6.0	−32.4	−0.31 (−1.20)	−0.50 (0.50)	−0.50 (0.50)
$^3O_2$ + $^-CH{-}CH{=}O$		2.5	−26.2[a]	−0.56 (0.11)	0.03 (1.04)	−0.14 (0.84)
		6.0	−31.6	−0.60 (0.0)	0.02 (1.020)	−0.02 (0.98)

a) −301.7063 a.u. by BSII.

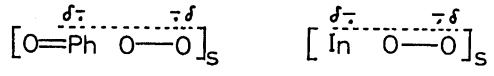

11 12

Chart 2.

from the potential curve in Fig. 8, the process in Eq. 16d should occur exclusively in the solution phase in accord with Adam's experiments.[35c]

CT Mechanism for Base-Catalyzed Oxygenations

1. Oxygenation Reactions via Charge-Transfer (CT) Complexes. The base-promoted oxygenation of phenol (PhOH) and indole (InH) derivatives were extensively studied.[17,18] These experiments have revealed that substrates are activated by bases as monoanion forms, which react with triplet molecular oxygen during the initial step. However, the experimental results show that the complete one-ET mechanism in Eq. 15a is not operative for these oxygenations, at least in a protic solvents, in contradiction to the preceding Russel mechanism.[21] Alternatively, a mechanism involving charge-transfer (CT) complexes[23,24] could be compatible with the available experimental results, particularly the regioselectivities, product distributions,[17] and kinetics (Chart 2).

$$PhO^- + {}^3O_2 \longrightarrow \mathbf{11} \longrightarrow O{=}PhOO^- \quad (17a)$$

$$In^- + {}^3O_2 \longrightarrow \mathbf{12} \longrightarrow InOO^- \quad (17b)$$

The ab initio and INDO calculations of molecular clusters comprising the phenoxide anion (or indole anion), molecular oxygen, and water molecules were carried out to elucidate the net charge transfers from the anion to triplet molecular oxygen associated with the hydrogen bondings of the water molecules. Figure 9 illustrates the approach models examined, where the three distances (R_1(X_1–O_2), R_2(O_2–O_3), and R_3(O_3–H_4)) are taken as variable parameters and the angles ($X_1O_2O_3$, $O_2O_3H_4$, and $O_3H_4O_5$) were fixed to be 120°, 109°, and 180°, respectively. Both the O-and C_4(para)-attacks of the phenoxide anion by triplet molecular oxygen were examined. The $\sigma\pi$ ET BR state was found to be the most stable among the four BR states in Fig. 6 in the region $R_1 > 2.0$ Å. Table 4 summarizes the net charge transfer (CT), net charges on the reaction centers, and the corresponding spin densities.

The O-attack shown in Fig. 9 was first examined. From Ao of Table 4, the net CT from the phenoxide anion to the triplet molecular oxygen is only 14%, even at R_1=2.0 Å, without the participation of water, and is negligible in the region $R_1 > 4.0$ Å. This implies that a one-electron transfer from the phenoxide anion to the triplet oxygen does not occur in a nonpolar solution. When a water is placed behind the oxygen so as to assist the CT its weight increase from 22 to 35% along with a decrease in the O_3–H_4 distance (R_3), which is responsible for the increase in the hydrogen bonding interaction. It becomes 68% at R_3=1.3 Å when the O–O length (R_2) is elongated to be 1.27 Å, which corresponds to that of the superoxide anion. Therefore, the CT complex (**13**) between the phenoxide anion and triplet molecular oxygen could be formed by elongation of the O–O bond and participation of a polar solvent (Chart 3). On the other hand, a complete one-electron transfer occurs even in the region $R_1 > 4.0$ Å, as shown in A_1 and A_2 of Table 4, when the H_4–O_3 distance (R_3) is shortened to be 1.21 Å. The back CT from the superoxide to the phenoxyl radical occurs at a relatively short O_2–O_3 distance (R_2) in the model. The net charge and spin-density populations show that the electronic structure of the reaction enters can be essentially regarded as an anion. This indicates that strong hydrogen bonding (or proton transfer) is extremely important for a complete one ET from the phenoxyl anion to the triplet oxygen, leading to the formation of radical pairs **14**.

Acceleration of the ET reaction was induced by the clustering of water molecules to the hydroxy anion, as illustrated in Fig. 9, where the geometry of the clusters was assumed to be the same as shown elsewhere.[36] The back CT from the superoxide anion to the phenoxyl radical, on the other hand, was suppressed by cluster formation. The present calculations show that the distinction between the CT complex formation and one ET reaction is very important, since in the former case the phenoxyl radical is not formed, while it could be released from the solvent cage in the latter case,

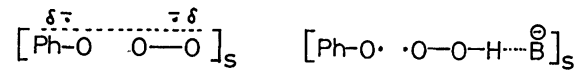

13 14

Chart 3.

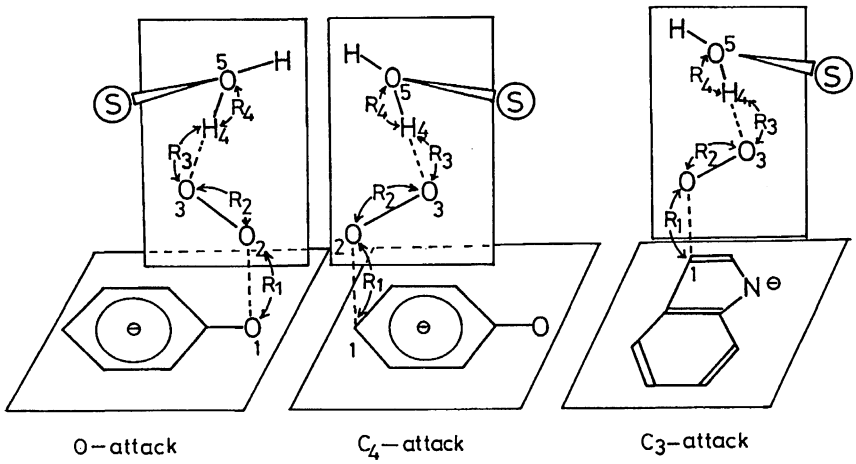

Fig. 9. Approach models of molecular oxygen plus solvent (S=H_2O) toward phenoxide and indole monoanions. Models A, B, and C denote the O^-- and C^- (*para*)-attacks of molecular oxygen to phenoxide anion, and C^- (3-position)-attacks of molecular oxygen to indole anion, respectively.

Table 4. Charge Transfer, CT (%), Net Charges (ΔP) and Spin Densities (ΔQ) for Phenolate Anion Plus $^3O_2\cdot(H_2O)_n$[a,b] and Indole Anion Plus $^3O_2\cdot(H_2O)_n$[c] Systems

No.	Distances			CT(%)	Net charges (Spin densities)				
	R_1	R_2	R_3		ΔP_1 (ΔQ_1)	ΔP_2 (ΔQ_2)	ΔP_3 (ΔQ_3)	ΔP_4 (ΔQ_4)	ΔP_5 (ΔQ_5)
A_0	2.0	1.207	—	14.67	−0.59 (0.19)	−0.01 (1.00)	−0.13 (0.86)	—	—
	3.0	1.207	—	0.03	−0.66 (0.00)	0.01 (1.03)	−0.03 (0.97)	—	—
	4.0—6.0	1.207	—	0.00	−0.66 (0.00)	0.01 (1.01)	−0.01 (0.99)	—	—
A_1	2.0	1.207	1.3	35.3	−0.49 (0.41)	−0.07 (0.94)	−0.19 (0.71)	0.26 (−0.01)	−0.47 (0.00)
	2.0	1.207	1.4	28.6	−0.52 (0.35)	−0.04 (0.96)	−0.17 (0.75)	0.24 (0.00)	−0.44 (0.00)
	2.0	1.207	1.6	21.8	−0.56 (0.27)	−0.03 (0.98)	−0.15 (0.80)	0.22 (0.00)	−0.40 (0.00)
	2.0	1.27	1.3	67.5	−0.34 (0.70)	−0.22 (0.80)	−0.33 (0.53)	0.27 (0.00)	−0.50 (0.00)
	3.0	1.27	1.3	0.02	−0.66 (0.00)	0.03 (1.01)	−0.02 (0.92)	0.22 (−0.07)	−0.39 (0.13)
	2.0	1.207	1.21	79.2	−0.29 (0.79)	−0.21 (0.80)	−0.31 (0.42)	0.25 (0.00)	−0.59 (0.00)
	3.0	1.207	1.21	99.9	−0.21 (0.93)	−0.32 (0.69)	−0.36 (0.34)	0.25 (0.00)	−0.62 (−0.02)
	5.0, 6.0	1.207	1.21	100	−0.21 (0.93)	−0.32 (−0.68)	−0.35 (0.34)	−0.25 (0.00)	−0.62 (−0.02)
A_2	2.0	1.207	1.21	81.7	−0.28 (0.81)	−0.21 (0.79)	−0.31 (0.40)	0.26 (0.00)	−0.60 (−0.02)
	3.0	1.207	1.21	99.9	−0.21 (0.93)	−0.31 (0.69)	−0.35 (0.33)	0.26 (0.00)	−0.62 (−0.02)
	5.0, 6.0	1.207	1.21	100	−0.21 (0.93)	0.31 (0.69)	−0.35 (0.34)	0.25 (0.00)	−0.62 (−0.02)
A_3	2.0	1.207	—	12.2 (4.9)[d]	−0.04 (−0.01)	−0.04 (0.96)	−0.88 (0.90)	—	—
	3.0—6.0	1.207	—	0.0	−0.09 (0.00)	0.01 (1.01)	−0.01 (1.00)	—	—
A_4	2.0	1.207	1.21	85.2	0.13 (0.15)	−0.27 (0.69)	−0.30 (0.42)	0.25 (0.00)	−0.59 (−0.02)
	3.0	1.207	1.21	99.8	0.05 (0.15)	−0.33 (0.67)	−0.35 (0.35)	0.25 (0.00)	−0.62 (−0.02)
	4.0—6.0	1.207	1.21	100	0.04 (0.15)	−0.32 (0.68)	−0.35 (0.35)	0.25 (0.00)	−0.62 (−0.02)
B_0	2.0	1.207	—	14.5 (7.6)[e]	−0.09 (0.02)	−0.03 (0.98)	−0.12 (0.87)	—	—
	3.0	1.207	—	0.17	−0.15 (0.00)	−0.02 (1.02)	−0.02 (0.97)	—	—
	4.0—6.0	1.207	—	0.00	−0.15 (0.00)	0.01 (1.01)	−0.01 (0.99)	—	—
B_1	2.0	1.207	1.21	33.1	−0.15 (0.13)	−0.03 (0.97)	−0.12 (0.69)	0.24 (−0.01)	−0.52 (0.02)
	3.0	1.207	1.21	0.14	−0.15 (0.00)	0.02 (0.99)	0.00 (0.83)	0.17 (−0.26)	−0.35 (0.46)
	4.0—6.0	1.207	1.21	0.00	−0.15 (0.00)	0.00 (0.97)	0.01 (0.83)	0.17 (−0.27)	−0.34 (0.49)
B_2	2.0	1.207	1.21	36.7	−0.04 (0.15)	−0.40 (0.96)	−0.13 (0.67)	0.25 (−0.01)	−0.53 (0.01)
	3.0	1.207	1.21	0.18	−0.15 (0.00)	0.03 (1.00)	0.01 (0.83)	0.18 (−0.25)	−0.37 (0.44)
	4.0—6.0	1.207	1.21	0.00	−0.15 (0.00)	0.01 (0.98)	0.01 (0.83)	0.18 (−0.26)	−0.35 (0.47)

a) O-attacks: $A_0(PhO^- + {}^3O_2)$, $A_1(PhO^- + {}^3O_2 + H_2O)$, and $A_2(PhO^- + {}^3O_2 + 2H_2O)$. b) C_4-attacks: $A_3(PhO^- + {}^3O_2)$ and $A_4(PhO^- + {}^3O_2 + H_2O)$. c) C_3-attacks: $B_0(In^- + {}^3O_2)$, $B_1(In^- + {}^3O_2 + H_2O)$, and $B_2(In^- + {}^3O_2 + 2H_2O)$. d) CT by the STO-3G (Et=−448.6138 a.u.). e) CT by the STO-3G (Et=−503.9110 a.u.).

leading to the radical chain process, namely, the so-called autoxidation via Russell mechanism in Eqs. 15a and 15b.[21]

Next, a C_4-attack of the phenoxyl anion was examined, as shown in Fig. 9. The calculated results are summarized in A_3–A_4 of Table 4. The CT character is only 20% even for the O–O elongated model (R_2=1.35 Å) assisted by hydrogen bonding (R_3=1.80 Å) (see Fig. 2). It increases with a decrease of the O_3–H_4 distance, suggesting CT complex formation **11** as in the case of an O-attack **13**. On the other hand, a complete one-electron (ET) transfer **15** occurs in the case of the protonated (or strong hydrogen bonding) model (R_3=1.21 Å) (Chart 4). The ab initio and INDO calculations indicate that the CT complex mechanism is operative for base-promoted oxygenations of the phenol derivatives in such aprotic solvents as DMF, while the one ET mechanism (i.e., free radical) is feasible in aqueous solution.

Similar calculations in indole anion, triplet oxygen and water systems were carried out, as illustrated in Fig. 9. The results given in Table 4 show that the maximum of the net electron transfer is only 37% even if the strong solvation by two water molecules is taken into account for the formation of a strong CT complex (**12**). A complete ET (**16**) did not occur even if the O–O bond of triplet oxygen was extremely elongated. These results indicate that free monoanions of indole derivatives are not very sensitive to triplet molecular oxygen.

From the above results, we can easily understand that ET biradical characters in the complexes between molecular oxygen and monoanions of phenol (or indole) are controlled by the magnitude of hydrogen bonding interactions. Therefore, we must investigate the charge-transfer interactions between these species in detail.

2. CT Mechanism for Oxygenations of Substituted Phenols and Indoles. We performed ab initio and INDO MO calculations which revealed two distinctive mechanisms for the initial step of base-promoted oxygenations: One is the autoxidation (radical chain) mechanism, which is initiated by a complete one electron-transfer form substrate anion to triplet molecular oxygen. The other is the CT complex mechanism, which is described below in detail (Chart 5). Needless to say, the ab initio post Hartree–Fock calculations involving electron correlation corrections are inevitable for depicting reliable potential curves in Figs. 5, 7, and 8 in order to elucidate the variations of the ET biradical characters with the intermolecular distances. Such reliable ab initio computations are also desirable to confirm the numerical results given in Table 4. However, they were hardly performed for the systems under examination at the present stage.[24]

Here, Mulliken's CT theory was alternately employed, since it enabled us to estimate the ET biradical character using the ionization or oxidation potential of the substrates.[24]

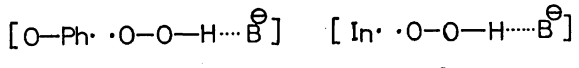

15 16

Chart 4.

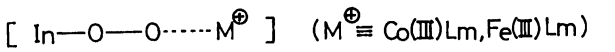

17

Chart 5.

As shown in the preceding MO calculations, the ^{3}CT configuration [D·O_2^-] is less stable than the configuration ^{3}A [D^- $^3O_2$] for triplet oxygen plus monoanions (D^-) of phenols and indoles at a relatively large intermolecular distance (R) of R_1>3.0 Å. Therefore, the formation of free superoxide anions is endothermic in these systems. However, the ^{3}CT configuration is not much destabilized with the decreasing intermolecular distance because of an increase in the electron-hole attraction, whereas the ground configurations (^{3}A) is destabilized by an increase in the exchange repulsion. Therefore, the ^{3}CT and ^{3}A configurations can be nearly degenerated in energy at a relatively shorter intermolecular distance. In such a situation, the triplet state of the CT complexes should be described by the superposition of both of these configurations,

$$^3\Phi_{CT} = C_0\,^3A + C_1\,^3CT \tag{18}$$

where C_0 and C_1 are obtained by solving the secular determinant. The ground-state stabilization energy (E_{total}) and CT excitation energy (ΔE_{CT}) are given as functions of (γ+E_s), as follows:

$$E^{\pm} = \frac{1}{2}\left\{(\gamma+E_s) \pm \sqrt{(\gamma+E_s)^2+4W^2}\right\} \tag{19}$$

$$\Delta E_{CT} = \sqrt{(\gamma+E_s)^2+4W^2}. \tag{20}$$

Here, E_s is the solvation energy difference between the ^{3}A and ^{3}CT configurations; γ is the energy difference between these configurations, and is approximately given by

$$\gamma = I_P - E_A + J_{AD}. \tag{21}$$

I_p and E_A are the ionization potential of the donor and electron affinity of triplet molecular oxygen, respectively. J_{AD} is the Coulombic attraction between the radical pairs [D·O_2^-]. W is an interaction term between the two configurations, and is proportional to the intermolecular orbital overlap. The stabilization energy (E_{total}) becomes larger if the solvation energy (E_s) is large and the γ-value is small. For a large E_s and small γ, E_{total} may well become large enough to outweigh the exchange repulsion energy. As a consequence, an intermediate with a strong CT character may be formed. The CT character (X_{CT}) is defined using the weight of the CT configuration in Eq. 18,

$$X_{CT} = C_1^2, \tag{22}$$

where the complete one ET BR corresponds to one of the extreme (X_{CT}=1), while the no ET state corresponds to the other extreme (X_{CT}=0). The functional dependences of E_{total}, ΔE_{CT}, and X_{CT} on (γ+E_s) are depicted in Figs. 10 and 11.

The relationships in Figs. 10 and 11 can be used to estimate the CT character for an initial complex with triplet spin multiplicity, i.e., a ^{3}CT complex. The spin inversion

of the complex is the crucial next step for forming a singlet organodioxide anion. To elucidate the electronic mechanism of this step, we consider an approach model between the phenoxyl anion and the triplet oxygen with C_s symmetry. The electronic structures of the ^{3}A and ^{3}CT configurations with the A symmetry are given by

$$^3\mathrm{A(A)} : \pi(\mathrm{PhO}^-)\bar{\pi}(\mathrm{PhO}^-)\pi_y^*(\mathrm{O_2})\pi_x^*(\mathrm{O_2}) \quad (23a)$$

and

$$^3\mathrm{CT(A)} : \pi(\mathrm{PhO}\cdot)\pi_y^*(\mathrm{O_2}^{-\cdot})\pi_x^*(\mathrm{O_2}^{-\cdot})\bar{\pi}_x^*(\mathrm{O_2}^{-\cdot}). \quad (23b)$$

These are schematically illustrated in Figs. 12A and 12B. The ground configuration (^{3}A) is the most stable at a relatively larger interatomic distance, whereas it is destabilized sharply at a smaller distance because of an exchange repulsion. On the other hand, the CT configuration is stabilized at an early stage, becoming more stable than the ^{3}A configuration. Therefore, an avoided crossing between the ^{3}A and ^{3}CT configurations occurs, as illustrated in Fig. 7B, leading to the formation of the ^{3}CT complex with a strong CT character on the ground triplet surface with A symmetry. In fact, the net charge transfers obtained by the MO calculations (Table 4) support strong configuration mixing. On the other hand, the local minimum on the excited A-state curve is regarded as a funnel, which allows ion annihilation, providing a phenoxide anion and triplet molecular oxygen:

$$^2\mathrm{PhO}\cdot + {}^2\mathrm{O_2}^{-\cdot} \longrightarrow {}^1\mathrm{PhO}^- + {}^3\mathrm{O_2} \quad (24)$$

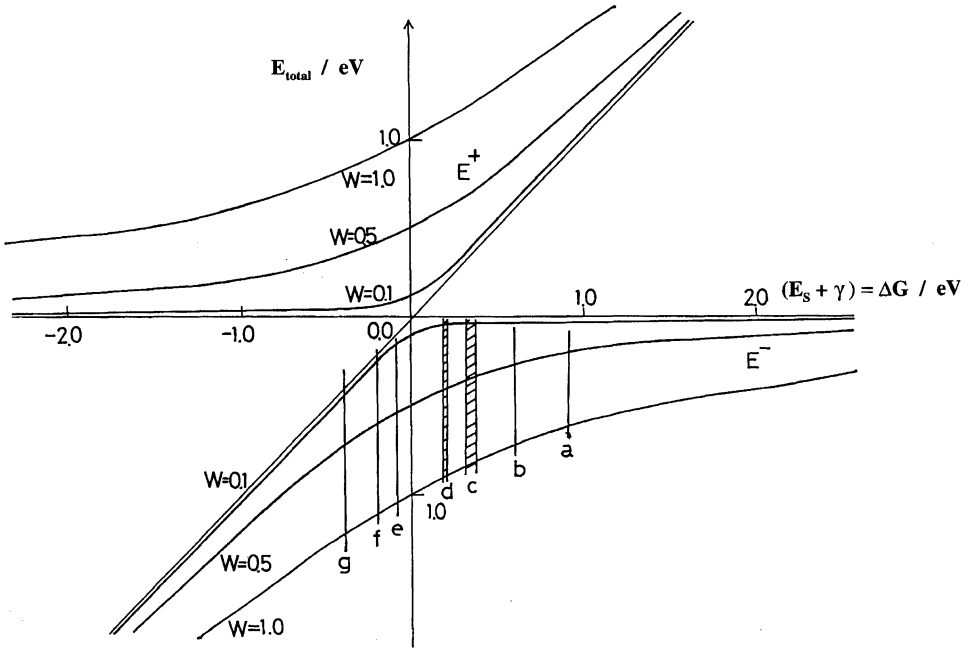

Fig. 10. Variations of the potential energy curves (Eq. 19) against the adiabatic energy difference ($E_S+\gamma$) between the ground and ^{3}CT configurations. W means the off-diagonal (interaction) term between these configurations. Some typical systems are given as follows: (a) NADH, (b) monoanion of 2,4,6-butylphenol, (c) flavin derivatives, (d) dianions of catechol derivatives with both O^-- and COO^--groups, (e) monoanions of 2,4,6-*t*-butylaniline, (f) dianion of indole, and triptamine derivatives with both the N^-- and 5-O^--groups and (g) dianions of catechol derivatives with two O^- groups.

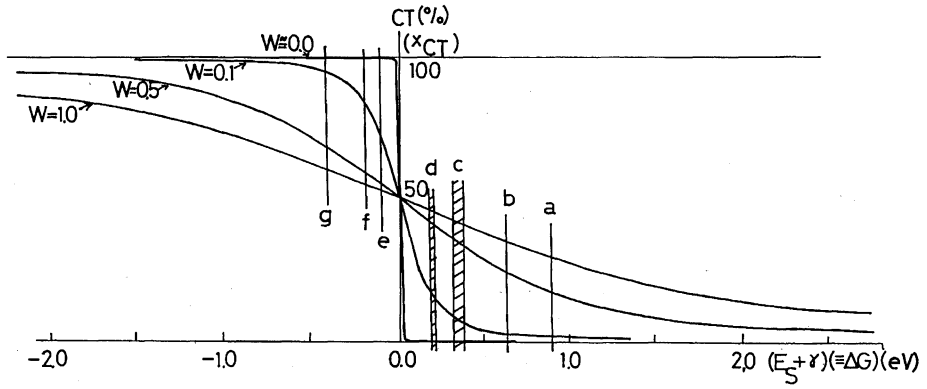

Fig. 11. Variations of the calculated CT characters (X_{CT} in Eq. 22) against the CT energy ΔG ($=E_S+\gamma$). The notations (a)—(g) are the same as those in Fig. 10.

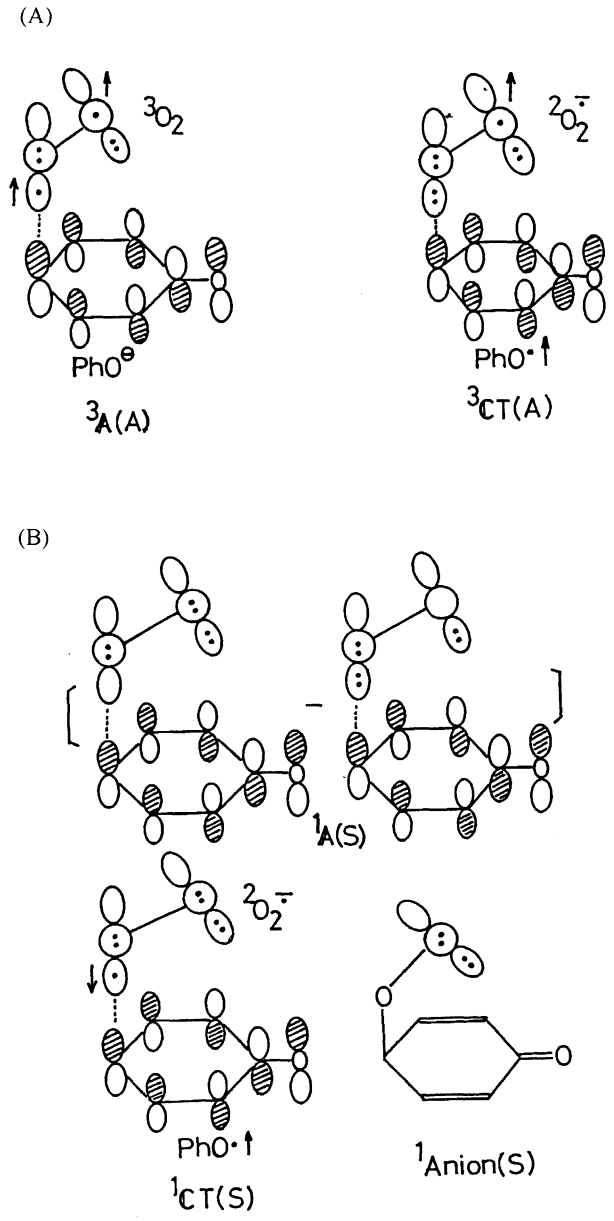

Fig. 12. (A) Orbital interactions between triplet molecular oxygen and phenoxide anion in the triplet no CT, ^{3}A, and ^{3}CT states; (B) Orbital interactions between singlet molecular oxygen and phenoxide anion in the singlet no CT, ^{1}A, and ^{1}CT states. S and A in parentheses denote symmetric and antisymmetric, respectively.

For converting the ground CT complex to a singlet anion, both spatial, and spin symmetry conversions are inevitable. Therefore, a singlet CT complex with the *S*-symmetry plays a crucial role in the process, since it correlates with the organodioxide anion. In fact, the CT (S) state is approximately described by the following two configurations:

$$^1\mathrm{A(S)} : \pi(\mathrm{PhO}^-)\bar{\pi}(\mathrm{PhO}^-)\pi_y^*(\mathrm{O_2})\bar{\pi}_y^*(\mathrm{O_2}) \tag{25a}$$

and

$$^1\mathrm{CT(S)} : \pi(\mathrm{PhO}\cdot)\pi_y^*(\mathrm{O_2}^{-\bullet})\bar{\pi}_y^*(\mathrm{O_2}^{-\bullet})\bar{\pi}_x^*(\mathrm{O_2}^{-\bullet}). \tag{25b}$$

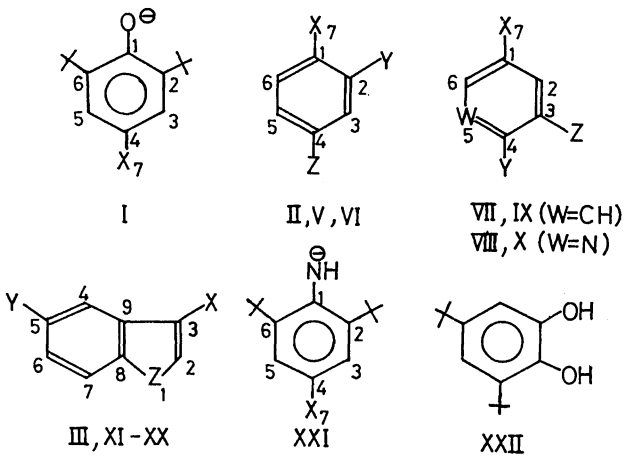

Fig. 13. Molecular structures of phenol, catechol, indole, and aniline derivatives which undergo base-prompted dioxygenetions.

Therefore, the spin-orbit (S.O.) coupling is highly effective at the surface crossing point, since the radical lobes are orthogonal to each other:

$$\langle {}^3\Phi_{\mathrm{CT}}|\mathrm{S.O.}|{}^1\Phi_{\mathrm{CT}}\rangle = k\langle\pi_x^*|\mathbf{l}|\pi_y^*\rangle\langle 1|\mathbf{s}|3\rangle \neq 0. \tag{26}$$

Thus, the reaction of the phenoxide anion with triplet molecular oxygen proceeds through the CT followed by a spin inversion (CTSI) mechanism.[22c] This reaction sequence is essentially the same even if the C_s symmetry restriction is removed out.

As previously discussed,[22] the CTSI mechanism thus involves two elementary steps: (1) one is the triplet CT complex formation; (2) the second is a spin inversion (SI) from the ^{3}CT complex to the ^{1}CT complex, followed by the formation of an organodioxide anion. The CTSI mechanism is applicable to many systems, for which complete one electron transfers are slightly endothermic. In fact, such situations hold for many important substrates (discussed below). Figure 7B illustrates possible potential curves concluded from Figs. 10 and 11. This shows the different features from the autoxidation surfaces in Fig. 7A.

3. Estimations of the CT Characters in Gas and Nonpolar Solutions. Figures 10 and 11 show that the weight (X_{CT}) of the CT configuration is essentially determined by the energy gap between the ^{3}A and ^{3}CT configurations, which is parallel to the ionization potential (I_P) of the donor anion, as shown in Eq. 21. Unfortunately, the gas-phase I_P's of monoanions of the phenol and indole derivatives have not yet been reported, although those of their neutral forms have been determined through UPS experiments by Houk et al.[37] and others.[38,39] Therefore, the I_P's of various phenol derivatives (**V**—**X** in Fig. 13) were calculated using the INDO method under the assumption

$$I_P = -\beta\varepsilon_{HO}, \tag{27}$$

where ε_{HO} means the orbital energy of the HOMO. The coefficient ($\beta(-0.762)$) was determined to reproduce the observed I_P's of **V**—**X** within ±0.3 eV. The ionization po-

Table 5. Ionization Potentials (I_P) and MO Coefficients of the HOMO's for Neutral, Monoanion, and Dianions of Phenol Derivatives

No.	Sub.			I_P	E_{OX}	MO Coefficients							
	X	Y	Z			1	2	3	4	5	6	7	8
IIa	OH	H	H	8.85	2.29	0.42	0.34	−0.19	−0.49	−0.20	0.34	−0.52	—
IIb	O^-	H	H	1.57	0.76	0.07	0.36	−0.03	−0.38	−0.03	0.36	−0.77	—
Va	OH	OH	H	8.24	1.68	0.42	0.42	0.11	−0.36	−0.36	0.11	−0.43	−0.43
Vb	O^-	OH	H	1.42	0.15	0.11	0.36	0.04	−0.37	−0.09	0.34	−0.75	−0.20
VIa	OH	OH	COOH	8.38	1.82	0.41	0.39	0.08	−0.37	−0.34	0.13	−0.41	−0.39
VIb	OH	OH	COO^-	4.91	1.00	0.44	0.33	−0.09	−0.39	−0.37	0.14	−0.36	−0.27
VIc	O^-	OH	COOH	1.99	0.32	0.08	0.35	0.08	−0.37	−0.05	0.34	−0.72	−0.20
VId	O^-	OH	COO^-	−1.28	−0.45	0.16	0.36	−0.01	−0.37	−0.13	0.33	−0.71	0.19
VIe	OH	O^-	COOH	1.75	0.26	0.35	0.11	0.35	−0.09	−0.36	0.04	−0.20	−0.75
VIf	OH	O^-	COO^-	−1.30	−0.45	0.36	0.14	0.33	−0.09	−0.38	−0.00	−0.21	−0.70
VIIa	OH	OH	H	8.03	1.47	0.42	0.27	−0.28	−0.42	−0.27	0.28	−0.42	0.42
VIIb	O^-	OH	H	1.39	−0.06	0.11	0.35	−0.08	−0.37	−0.08	0.35	−0.74	0.19
VIIc	O^-	O^-	H	−3.58	−1.20	0.26	0.27	−0.27	−0.26	−0.27	0.27	−0.54	0.54
VIIIa	OH	OH	H	8.17	1.61	0.43	−0.25	−0.28	−0.41	−0.29	0.29	−0.42	0.40
VIIIb	O^-	OH	H	1.39	0.05	0.12	0.34	−0.09	−0.36	−0.09	0.36	−0.75	0.19
VIIIc	OH	O^-	H	1.66	0.11	0.37	0.05	−0.35	−0.10	−0.39	0.12	−0.20	0.72
IXa	OH	OH	COOH	8.23	1.67	0.41	0.25	−0.29	−0.41	−0.25	0.28	−0.41	0.41
IXb	OH	OH	COO^-	4.75	0.84	0.38	0.08	−0.34	−0.43	−0.21	0.34	−0.32	0.41
IXc	O^-	OH	COOH	1.75	0.11	0.10	0.36	−0.08	−0.36	−0.08	0.34	−0.75	0.19
IXd	O^-	OH	COO^-	−1.39	−0.63	0.14	0.33	−0.08	−0.38	−0.12	0.36	−0.73	0.21
IXe	OH	O^-	COOH	1.94	0.12	0.37	0.12	−0.35	−0.08	−0.34	0.05	−0.20	0.72
IXf	OH	O^-	COO^-	−1.77	−0.61	0.37	0.02	−0.35	−0.10	−0.35	0.10	−0.17	0.73
Xa	OH	H	COOH	8.82	2.26	0.40	0.16	−0.32	−0.42	−0.01	0.42	−0.45	—
Xb	OH	H	COO^-	5.33	1.53	0.32	−0.07	−0.37	−0.43	0.05	0.47	−0.29	—
Xc	O^-	H	COOH	1.94	0.73	0.09	0.35	−0.05	−0.36	−0.02	0.36	−0.77	—

tentials of the monoanions and dianions of **V**—**X** were also calculated using the same equation. The calculated I_P's of neutral, monoanions and dianions of **V**—**X** are summarized in Table 5, together with the MO coefficients of the HOMO's. The same procedures were applied to neutral and anion forms of indole derivatives (**III**,**XI**—**XX**) in Fig. 13. The results are given in Table 6.

The I_P's of the phenol derivatives (**V**—**X**) are reduced by about 6.5—7.5 eV along with the deprotonation of OH. Therefore, deprotonations of the species catalyzed by bases lead to a paramount increase in their reactivities to triplet molecular oxygen. However, the shapes of the HOMO's are not drastically changed by the deprotonation, as shown in Table 5, indicating the greater reactivities of the *para*- and *ortho*-positions than the *meta*-position for electrophilic reagents, such as $^3O_2$. Therefore, the regioselectivities in the electrophilic reactions of phenol derivatives are not changed upon the deprotonation of OH. The I_P's of catechol analogs **VI, IX**, and **X** are not very much changed by introducing a carboxyl group, whereas they are reduced by about 3.5 eV with the deprotonation of COOH. This implies that the deprotonation of the side COOH group in catechol derivatives could be a trigger to induce complete one-electron transfer reactions. In fact, the I_P's of the dianions of catechol derivatives in the gas phase were calculated to be largely negative in sign under the present approximation. Judging from the LCAO coefficients in Table 5, the shape of the HOMO is not very much changed by the deprotonation of COOH or OH in the system.

The I_P's of the indole derivatives are reduced by about 5.2—5.9 eV with the deprotonation of NH, indicating a drastic increase in their reactivities to electrophilic reagents. The greater electrophilic reactivity of the 3-position than the 2-position is not changed upon deprotonation, as shown in Table 6. The deprotonation of OH at the 5-position of **XIV** reduced the I_P by 3 eV. The I_P of the dianion **XIVc** is therefore negative in sign as in, the case of catechol dianions.

The CT energy (γ) is estimated using the calculated I_P's of the phenoxide and indole monoanions, assuming that J_{AD} in Eq. 21 is zero. Table 7 summarizes the E_A-values of some oxygen-centered radicals and corresponding γ-values for phenoxide (**II**) and iondole (**III**) monoanions. The complete one-ET reaction from phenoxide and indole monoanions to triplet molecular oxygen is endothermic by 1.13 and 1.57 (eV), respectively. Although the ET reaction with hydroperoxyl radicals is exothermic for phenoxide anion, it is endothermic for the indole anion. The results are wholly compatible with the preceding MO calculations. From the I_P's given in Table 5, one-ET reaction toward triplet molecular oxygen is endothermic for other monoanions of phenol and its derivatives in gas phase. The ^{3}CT characters of the gas-phase CT complexes are small, as can be recognized from the γ-values. On the other hand, the one ET reaction is largely exothermic for all of the dianions of the phenol and indole derivatives examined here. Interestingly, the one ET reaction is facile for dianions formed by the deprotonations of OH and COOH of catechol derivatives in the gas phase and nonpolar solutions.

Table 6. Ionization Potentials (I_P) and MO Coefficients of the HOMO's for Neutral, Monoion, and Dianions of Indol and Triptamine Derivatives

No.	Sub.			I_P	E_{OX}	MO Coefficients								
	X	Y	Z			1	2	3	4	5	6	7	8	9
IIIa	H	H	NH	7.91	1.35	−0.52	0.25	0.46	−0.41	−0.23	0.26	0.41	−0.03	−0.03
IIIb	H	H	N^-	2.01	−0.18	−0.66	−0.03	0.48	−0.23	−0.28	0.16	0.32	−0.10	0.23
XIa	H	CH3	NH	7.78	1.22	−0.55	0.13	0.40	−0.41	−0.34	0.11	0.41	0.12	0.09
XIb	H	CH3	N^-	2.05	−0.31	−0.66	−0.04	0.46	−0.24	−0.30	0.14	0.32	−0.09	0.25
XIIa	H	OCH3	NH	7.37	0.81	−0.43	−0.06	0.23	−0.38	−0.36	−0.14	0.30	0.29	0.20
XIIb	H	OCH3	N^-	1.99	−0.72	−0.65	−0.08	0.44	−0.26	−0.31	0.08	0.31	−0.03	0.27
XIIIa	H	OH	NH	7.55	0.99	−0.55	−0.02	0.29	−0.40	−0.38	−0.07	0.35	0.26	0.19
XIIIa	H	OH	N^-	1.90	−0.54	−0.65	−0.08	0.44	−0.26	−0.31	0.08	0.32	−0.03	0.27
XIVa	H	O^-	NH	4.40	0.25	−0.37	0.36	0.41	−0.38	−0.07	0.41	0.39	−0.18	−0.25
XIVb	H	O^-	NH	1.26	−0.49	−0.21	−0.08	0.12	−0.41	−0.11	−0.30	0.09	0.33	−0.08
XIVc	H	O^-	N^-	−0.95	−1.01	−0.48	0.22	0.50	−0.14	−0.04	0.41	0.22	−0.34	−0.05
XVa	$(CH_2)_2NH_2$	H	NH	7.70	1.14	0.47	0.30	−0.52	0.36	0.24	−0.21	−0.36	−0.01	−0.05
XVb	$(CH_2)_2NH_2$	H	N^-	2.10	−0.39	0.49	0.00	−0.64	0.31	0.17	−0.26	−0.23	0.22	−0.12
XVIa	$(CH_2)_2NHCH_3$	H	NH	7.71	1.15	0.47	0.30	−0.52	0.36	0.24	−0.21	−0.36	−0.01	−0.05
XVIb	$(CH_2)_2NHCH_3$	H	N^-	2.14	−0.38	0.49	0.00	−0.64	0.31	0.17	−0.26	−0.23	0.22	−0.12
XVIIa	$(CH_2)_2N(CH_3)_2$	H	NH	7.70	1.14	0.47	0.30	−0.52	0.36	0.24	−0.21	−0.36	−0.01	−0.05
XVIIb	$(CH_2)_2N(CH_3)_2$	H	N^-	2.14	−0.39	0.49	0.00	−0.64	0.31	0.17	−0.27	−0.23	0.22	−0.11
XVIIIa	$(CH_2)_2NH_2$	CH_3	NH	7.60	1.04	0.44	0.22	−0.54	0.37	0.15	−0.29	−0.38	−0.07	−0.04
XVIIIb	$(CH_2)_2NH_2$	CH_3	N^-	2.14	−0.49	0.48	0.01	−0.63	0.31	0.15	−0.28	−0.24	0.23	−0.10
XIXa	$(CH_2)_2NH_2$	OCH_3	NH	7.31	0.75	0.29	0.02	−0.47	0.31	−0.09	−0.34	−0.39	0.18	0.24
XIXb	$(CH_2)_2NH_2$	OCH_3	N^-	2.10	−0.78	0.46	−0.05	−0.63	0.30	0.09	−0.29	−0.26	0.26	−0.05
XXb	$(CH_2)_2N(CH_3)_2$	OCH_3	NH	7.32	0.76	0.29	0.02	−0.47	0.31	−0.09	−0.34	−0.38	0.18	0.24
XXb	$(CH_2)_2N(CH_3)_2$	OCH_3	N^-	2.14	−0.77	0.46	−0.05	−0.63	0.30	0.09	−0.29	−0.26	0.26	−0.04

Table 7. Charge-Transfer Energies of Phenol and Indole Anions to ^3O Oxygen Radicals

Oxygen radicals	E_A	$\gamma(PhO^-)$	$\gamma(In^-)$
O_2	0.44	1.13	1.57
O	1.46	0.11	0.44
OH	1.83	−0.26	0.18
CH_3O	1.8	−0.2	0.2
n-PrO	1.9	−0.3	0.1
HO_2	1.85	−0.28	0.16
O_3	2.89	−1.32	−0.88
RO_2	1.85	−0.28	0.16

4. Estimations of the CT Characters in Polar Solutions. Mono- and di-anions of phenol and indole derivatives are largely stabilized by solvations in polar solutions. Therefore, the one ET vs. CT reactions from these species to molecular oxygen might be controlled by selecting appropriate solvents. Rhem and Weller[40] have investigated the ET reactions on kinetic and thermodynamic grounds. The free-energy change for the production of the radical pair S· and $O_2^{-\cdot}$ in acrylonitrile is given by

$$\Delta G = E_{1/2}(S\cdot/S^-)_s - E_{1/2}(O_2^{-\cdot}/^3O_2) - e/a\varepsilon. \quad (28)$$

Here, $E_{1/2}$ ($S\cdot/S^-$) and $E_{1/2}$ ($O_2^{-\cdot}/^3O_2$) are the oxidation potential of the substrate anions S^- and the reduction potential of $^3O_2$ in the solvent, respectively. The last term is the Coulomb interaction between the radicals at the intermolecular distance (a) in a solvent of dielectric constant ε. Both the reduction and oxidation potentials in Eq. 28 implicitly involve not only the solvation energy, but also the entropy term. Thus, the ΔG is approximated by ($\gamma+E_s$).

The free-energy changes for electron transfers from monoanions of phenol derivatives were estimated using the observed oxidation potential (−0.2 SCE in MeCN) of the monoanion of 2,4,6-tri-*t*-butyl phenol (**Id**) as a reference.[41] The decrease in the oxidation potential of **Id** by deprotonation is only 1.53 eV. Therefore, the oxidation potentials (E_{OX}) of the other monoanions of phenol and indole derivatives can be approximately estimated from the observed E_{OX} of the neutral forms by

$$E_{OX}[S^-] = E_{OX}[SH] - 1.53. \quad (29)$$

The oxidation potentials probably involve the stabilization energies (E_s) of the substrate anion (S^-) with MeCN. The oxidation potential (E_{OX}) [SCE/MeCN] of the neutral form of **Id** is formally related to its observed ionization potential (I_P) as

$$E_{OX}[SH] = I_p(gas) - 6.56. \quad (30)$$

The oxidation potentials (E_{OX}) of other anions and dianions were not determined experimentally, and were, therefore, estimated by their calculated I_P's, assuming the following linear relationship:

$$E_{OX} = bI_p(gas) + c, \quad (31)$$

where the parameters (b and c) were determined so as to reproduce the E_{OX} values given by Eqs. 29 and 30. The b-value was found to be almost constant [b=0.23] for phenol

and indole derivatives. The calculated E_{OX} are summarized in Tables 5 and 6.

The free energies (ΔG) calculated for the neutral and monoanions of the phenol derivatives remain positive, as shown in Table 5, indicating that the one-ET reactions are impossible, even in MeCN. Although the dianions generated by the deprotonations of OH and COOH, on the other hand, have negative E_{OX} values, the free energies are still positive in sign. Although the one-ET reactions are not favorable, CT complex formations are feasible, as can be recognized from the small magnitude of the ΔG values. Therefore, the CT complex mechanism could be operative for the oxygenations of these dianion species [–OPhCOO–] in a protic polar solutions (Chart 6). The one-ET and CT mechanisms, on the other hand, compete for these species in a protic or aqueous solution, since the ΔG-values in MeCN are reduced by 0.2—0.3 in the latter solution. The catechol dianions generated by the deprotonations of two OH groups have large negative E_{OX} values (<-1.0). Complete one-ET reactions are feasible for these species in polar solutions. However, the one-ET reactions might be suppressed in the case of metal-catalyzed oxygenations, since the metal ions largely stabilize the an ions **19**, **21**, and **22** (Chart 7).[10a,33] Successive decompositions of **19**, **21**, and **22**have already been investigated by Foote et al.[42] and Nozaki et al.[43]

From Table 6, although the monoanions of indole and triptamine have small negative E_{OX} values, the ΔG-values for theses species maintain a positive sign. Therefore, the CT complex mechanism could be operative for the oxygenations of monoanions of indole and tryptamine. The ΔG-values become almost zero for their 5-MeO derivatives. Both one-ET and CT mechanisms may compete in oxygenations of the species, even in MeCN. On the other hand, the ΔG-values are negative for dianions formed by the deprotonations of 5-OH, indicating that the one-ET mechanism is feasible. Thus, the roles of metal ions seem to be essential for controlling the one-ET vs. CT processes in the oxygenation reactions of indole derivatives[3,9,33]

CT and One-ET Mechanisms for Phenol, Aniline, and Flavin Derivatives

The base-promoted dioxygenations of phenols and indoles are none other than the dioxygen incorporation into carbanions generated in the aromatic rings through a resonance.

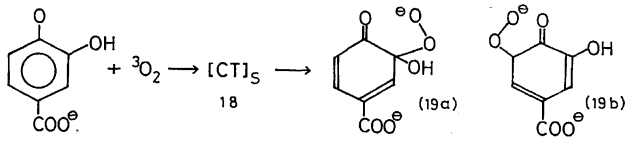

Chart 6.

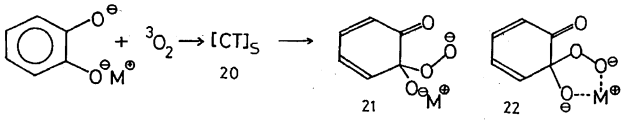

Chart 7.

As described above, the dioxygenation of a simple carbanion involves a one-electron transfer (ET) from the carbanion to triplet molecular oxygen, and proceeds by a radical chain mechanism.[20,21] Formally, a bimolecular nonradical mechanism for the formation of singlet hydroperoxides by the reaction of singlet substrates with triplet molecular oxygen has been excluded based on a spin-conservation rule.[44] The present MO plus intermolecular CI model calculations, however, indicated that the nonradical process for the dioxygenation can be rationalized by considering CT complex intermediates, whose formations depend on the redox potentials of the phenoxide and indole anions employed. The present theory also indicates that deprotonation from protic substrates lowers the redox potentials of the substrates, promoting an interaction between the substances and triplet molecular oxygen to form triplet CT complexes, which can undergo spin inversions to singlet CT complexes, as illustrated in Fig. 7B. In this section we examine various experimental results in light of the theoretical conclusions given in the preceding sections.

1. Oxygenations of Phenol Derivatives. Nishinaga and his collaborators[17] have carried out systematic and extensive experimental studies on based-catalyzed oxygenations of phenol and indole derivatives. Scheme 1 summarizes the experimental results. *t*-BuOK and Co^{III}(salpr)(OH) promote the oxygenation of 2,6-di-*t*-butylphenols (**23**), resulting in regiospecific dioxygen incorporation, depending on the nature of the substituent at the 4-position as well as the reaction conditions:[17] The oxygenation of **23** (Z=alkyl) with *t*-BuOK in *N*,*N*-dimethylformamide (DMF), where the phenoxide anion is in a free state, results in exclusive dioxygen incorporation into the *para* position, finally to give epoxy-*p*-quinols **25**) (Z=alkyl), whereas under these conditions phenols **23** (Z=Ar, COR) are not reactive.

The *para*-attack in **23** (Z=alkyl) is consistent with the LCAO coefficient of HOMO in Table 5, and the decrease of the electrophilic reactivity by introducing an electron-withdrawing group is reasonable. On the other hand, phenols **23** (Z=Ar) can undergo oxygenation with *t*-BuOK in *t*-BuOH, where the phenoxide anion is associated with K^+, resulting in exclusive dioxygen incorporation into the *ortho* position to give **24** (Z=Ar). Phenols bearing an electron-withdrawing group (**23**; Z=COR, CN, etc.) are no longer susceptible to the *t*-BuOK-promoted oxygenation system, but are oxygenated in the presence of Co^{III}(salpr)(OH) in CH_2Cl_2 exclusively to give **26**. These gegen cation effects are also rationalyzed from Fig. 5A and the CT characters in Table 1. The regiospecificity for the dioxygenation of phenols **23** in the O_2/*t*-BuOK/*t*-BuOH system is the same as that in the O_2/Co^{III}(salpr)(OH)/CH_2Cl_2 system.[17c,17e,17g,17h,17i] This regiospecificity was found to be well correlated to the formal potential (E°) of the **23**–/**23**· redox couple, as illustrated in Fig. 14: The E° values of **23** (Z=alkyl) are below -654 mV, those of **23** (Z=aryl) are between -650 and -300 mV, and those of **23** (Z=COR, CN) are above -200 mV.[17a] The ortho dioxygenation takes place for **23** ($E^\circ > -645$ mV), whereas the para dioxygenation for **23** takes place with $E^\circ < -650$.

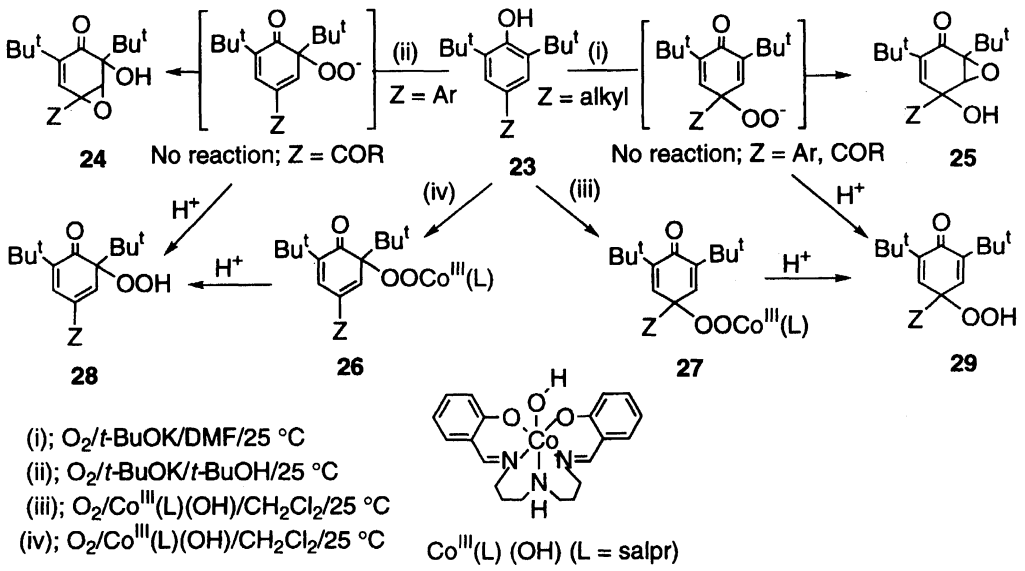

Scheme 1.

Interestingly, all of the phenoxide anions $\mathbf{23}^-$, whose $E°$ values are above −650 mV, do not undergo dioxygenation in DMF. In other words, these phenoxide anions are not susceptible to oxygenation in a free state, but in an associated form with a counter cation, K^+ or $[Co^{III}]^+$. Further, when the $E°$ value of $\mathbf{23}^-$ reaches a more positive value than −200 mV, oxygenation takes place only when it is associated with $[Co^{III}]^+$.

An interesting thing is that the Co^{III}(salpr)(OH)-promoted oxygenation of **23** results in the same regioselectivity as that observed for *t*-BuOK-promoted oxygenation (Scheme 1). In addition, even phenols, which are quite insusceptible to the *t*-BuOK/*t*-BuOH system, can be oxygenated by the promotion of Co^{III}(salpr)(OH). All of these experiments clearly indicate that the reaction modes can be controlled by the oxidation potentials and gegen cations; thus, Eqs. 28, 29, 30, and 31 associated with the numerical data in Tables 5 and 6 are quite consistent with the observations. Since the magnitudes of the LCAO coefficients in the *para*- and *ortho*-position of phenol derivatives are not very different, the difference in the reactivity between the *ortho*- and *para*-positions may be ascribed to a Coulombic field effect of the gegen ions.

The treatment of hydroperoxides **28** and **29** with *t*-BuOK in DMF under a nitrogen stream at room temperature, where the resulting organodioxide anions are in free state, gives phenoxide anions $\mathbf{23}^-$ in nearly quantitative yield, accompanied by the liberation of triplet molecular oxygen,[17f,17g,17j] whereas under an oxygen atmosphere epoxy-*p*-quinols **25** are formed quantitatively from **23** (Z=alkyl) and no reaction takes place with **23** (Z=Aryl, COR). These results suggest that the formation of organodioxide anions, $\mathbf{28}^-$ and $\mathbf{29}^-$, is a reversible process, and the equilibrium is shifted extremely to the starting system when the anionic species are in free states. These characteristices are rationalyzed from Fig. 7B, where the CT states are not very stabilized because of no gegen ion. On the other hand, when **29** (Z=*t*-Bu, Ar) was treated with *t*-BuOK in *t*-BuOH, where the resulting organodioxide anion is associated with K^+ in a solvent cage, the hydroperoxyl group migrates efficiently to the ortho position, giving rise to **28**, which is also obtained selectively by the oxygenation of **23** (Z=*t*-Bu, Ar) with *t*-BuOK in *t*-BuOH.[17] Interestingly, when KO_2 is reacted with phenoxyl radicals **23·** (Z=*t*-Bu, Ar) in DMF or in *t*-BuOH at room temperature, a complete electron transfer occurs from O_2^- to **23·**, giving rise to $\mathbf{23}^-$ and the ground state of $^3O_2$; however, no coupling takes place between them.[17] From these observations, it is reasonable to assume that the *t*-BuOK-promoted oxygenation of **23** does not involve radical intermediates **23˙**, but CT intermediates, as depicted in Fig. 7B.

Scheme 2 illustrates possible processes in the base-catalyzed oxygenations of phenol derivatives. From Scheme 2, the free form of the organodioxide anion $\mathbf{29}^-$ is too unstable to undergo an intramolecular decomposition, finally giving rise to epoxy-*p*-quinol **25** under an oxygen atmosphere; in its associated form $[\mathbf{23}^-K^+]$, however, the decomposition is slow and the *para–ortho* migration of the hydroperoxyl group within the CT complex occurs preferentially. Thus, migration may be promoted by a stabilization effect due to the chelate structure of the organodioxide anion $[\mathbf{28}^-K^+]$. The reaction of KO_2 with **23·** indicates that the reaction takes place in the excited state of the CT complex and, therefore, the reverse process, CT=**23·**+O_2^-, is energetically unfavorable, in accord with the present model calculations given in Fig. 7B and the numerical data in Tables 5 and 6.

Sheldon and Kochi[4] have discussed the possibility of the involvement of a phenoxyl radical intermediate in the oxygenation of **23** with Co(salpr). Since the $E°$ value of Co(salpr) is more positive than that of $\mathbf{23}^-$ (Z=alkyl) (see Fig. 14) and the oxygenation of **23·** (Z=alkyl) is faster than that of $\mathbf{23}^-$ (Z=alkyl),[17k] it may be reasonable to consider that the oxygenation of Co^{III}(salpr)($\mathbf{23}^-$) (Z=alkyl) involves **23·** (Z=alkyl) as an intermediate, where O_2 is always incorporated into the para position of **23**. On the other hand, from the data given in Fig. 14, the equilibrium constant for the

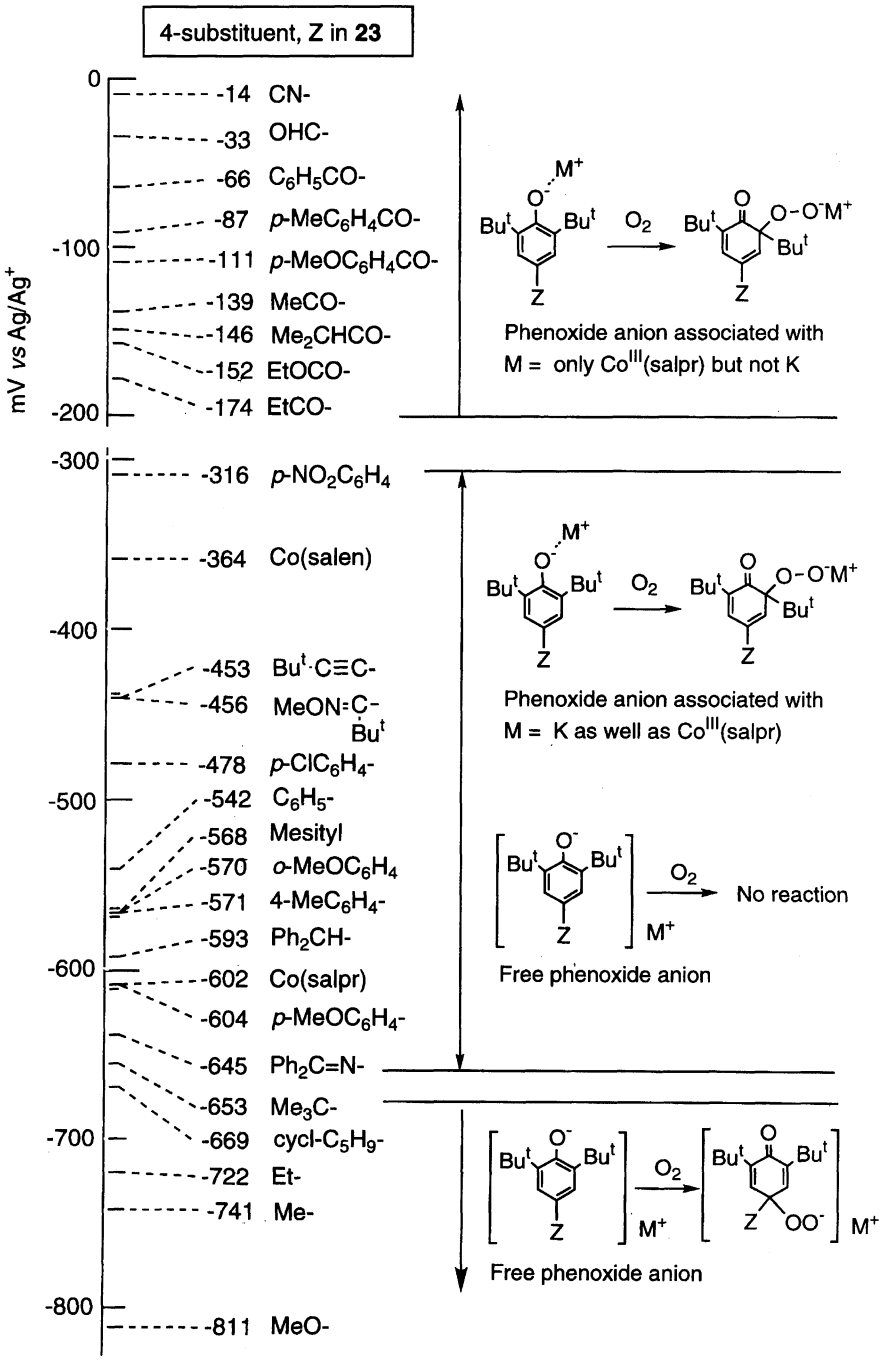

Fig. 14. Formal potential of $\mathbf{23}^-/\mathbf{23}\cdot$ redox couple for **23**. Conditions: 0.1 M NBu_4PF_6 in DMF. E_O: mean value of oxidation and reduction peak potentials, which are obtained at scan rates v=50—200 mV s^{-1}.

electron-transfer equilibrium between $[Co^{III}(salpr)]^+$ and $\mathbf{23}^-$ (Z=COMe), giving rise to $Co^{II}(salpr)$ and $\mathbf{23}\cdot$ (Z=COMe) was calculated to be about 1×10^{-8}; the concentration of $\mathbf{23}\cdot$ (Z=COMe) is about 1×10^{-4}%. Actually, very weak EPR signals for $\mathbf{23}\cdot$ (Z=COMe) (a triplet due to the ring protons) were detected in a solution of $[Co^{III}(salpr)(\mathbf{23}^-)$ (Z=COMe)] in CH_2Cl_2. However, the oxygenation of $Co^{III}(salpr)(\mathbf{23}^-)$ (Z=COMe), derived from the reaction of **23** (Z=COMe) with $Co^{III}(salpr)(OH)$, in CH_2Cl_2 was faster than that of $\mathbf{23}\cdot$ (Z=COMe) in CH_2Cl_2. Figure 15 shows the experimental data for the kinetics. Furthermore, the oxygenation of $\mathbf{23}\cdot$ (Z=COMe) gave 2,6-di-*t*-butyl-*p*-benzoquinone as the sole product. These results clearly indicate that no radical intermediate is involved in the oxygenation of $Co^{III}(salpr)(\mathbf{23}^-)$ (Z=COMe) in CH_2Cl_2, contrary to the argument by Sheldon and Kochi.[4]

Since no oxygenation of $Co^{III}(salpr)(\mathbf{23}^-)$ (Z=COMe) takes place in DMF, where $Co^{III}(salpr)(\mathbf{23}^-)$ (Z=COMe, CN) is dissociated to $[Co^{III}(salpr)]^+$ and $\mathbf{23}^-$; as judged by CV, the association form of $Co^{III}(salpr)(\mathbf{23}^-)$ is essential for oxygenation to take place. Similar results were obtained with $Co^{III}(salpr)(\mathbf{23}^-)$ (Z=Ar). Thus, the experimental results

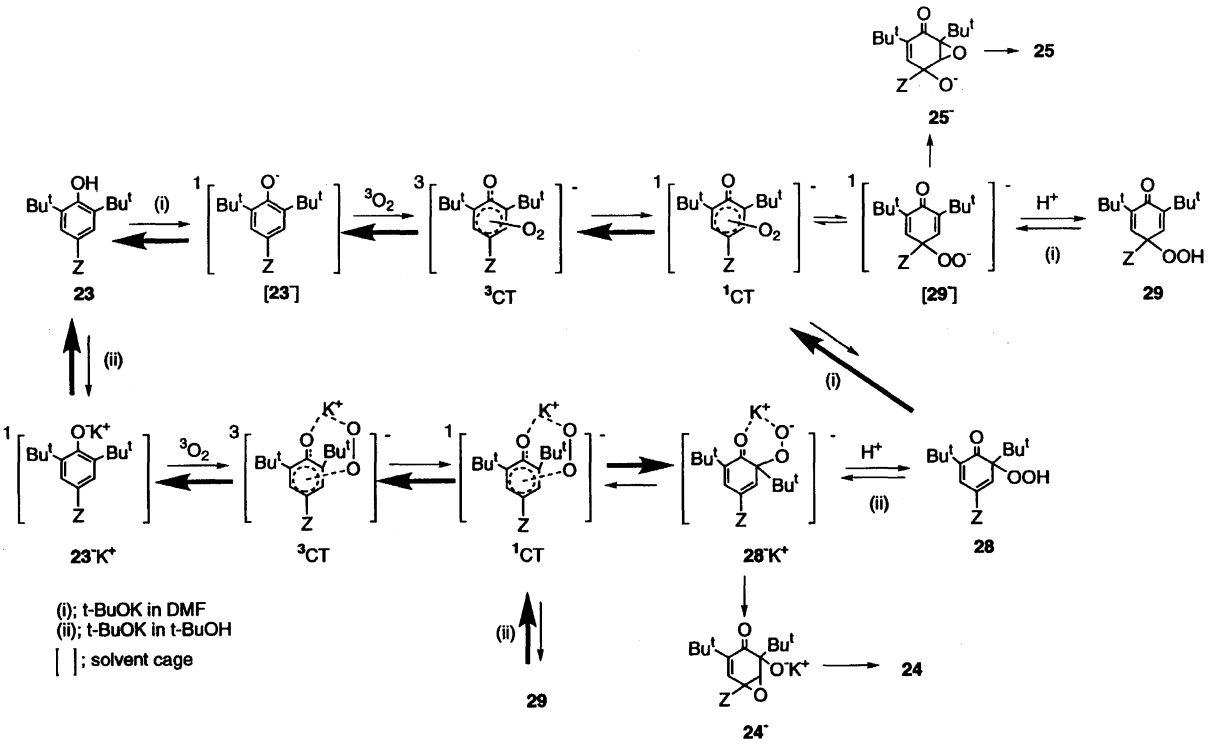

Scheme 2.

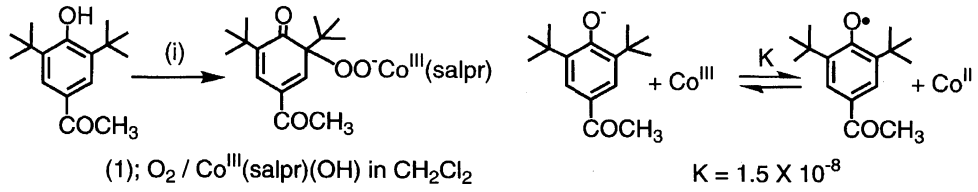

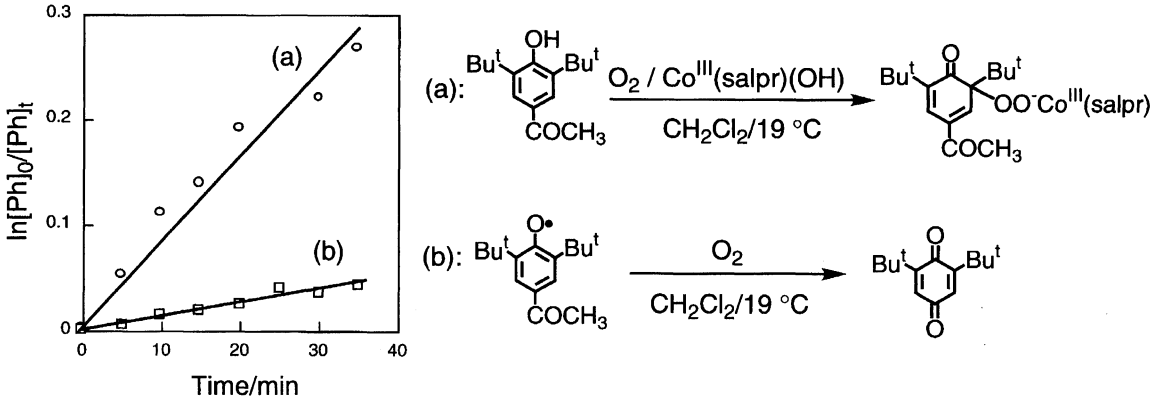

Fig. 15. Time course and product for the oxygenation of **23** (Z=CN) (0.1 M) with CoIII(salpr)(OH) (0.1M) and of **23**· (0.1 M) in CH_2Cl_2 (10 ml).

linked with the present computational results lead to the conclusion that the oxygenation process of **23** can be summarized as depicted in Scheme 3, and that is should be reasonable to assume a ternary complex (**28**) involving $\mathbf{23}^-$, O_2, and $[Co^{III}]^+$ as the transition state, which undergoes intersystem crossing under the influence of the Lewis acidity of $[Co^{III}]^+$, for the nonradical process. The entirely same type of activation process was also demonstrated for a model reaction using Co^{III}(SB)(OH) (SB=Schiff base) of quercetinase, one of dioxygenases.[19]

2. Oxygenation of Indole and Related Species. The present calculations predict that monoanions of indole derivatives are not sensitive to triplet molecular oxygen (vide supra). Actually, 3-substituted indoles are normally insusceptible to normal base-promoted oxygenation. However, these species are readily oxygenated by the catalysis of Co(Salen)(OH), a hydroxocobalt (**III** in Fig. 13) complex: Salen=*N*,*N*′-disalicylideneethylenediamine, resulting in the

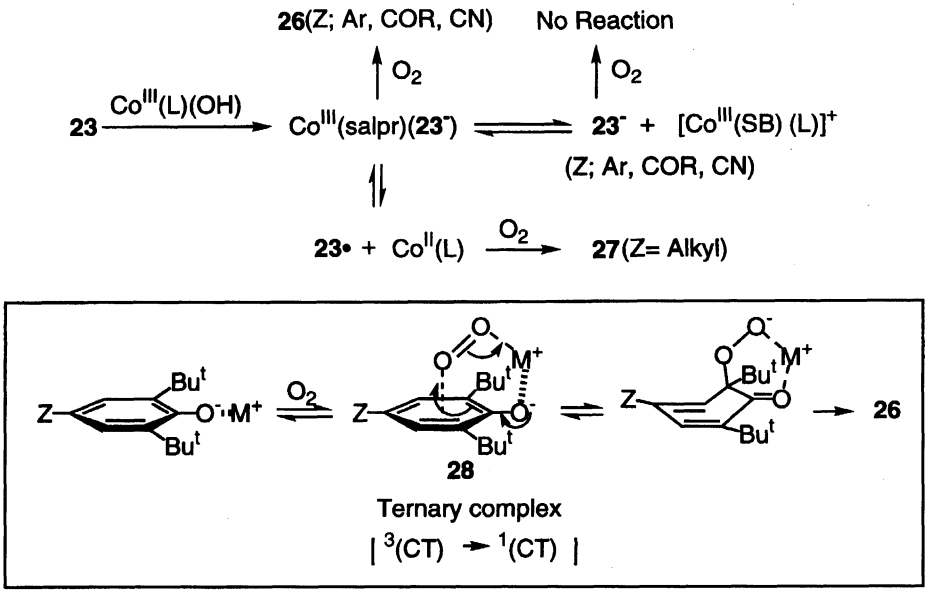

Scheme 3.

dioxygenolysis of the heterocyclic ring to give *o*-formylaminoacetophenone derivatives, where the cobalt complex functions as a base.[16b] The mechanism of these reactions can be rationalized in a similar manner in the case of phenol derivatives (**I**). From these observations, the important role of the transition metal ions is found to be

$$S^- + {}^3O_2 \longrightarrow {}^3(CT) \xrightarrow{M^+} {}^1(CT) \xrightarrow{M^+} [SOO^-M^+] \quad (32)$$

The oxidation potentials for the monoanions of various phenol and catechol derivatives and indole derivatives in Tables 5 and 6 are consistent with the above CT mechanism. The relations of these species to the biological systems are interesting problems which will be solved in the future.

In contrast to phenoxide and indole monoanions, the calculated free energies for 4-substituted 2,6-di-*t*-butylanilines (**XXI**) become negative in sign in an aprotic solvent, as shown in Table 8. The one-ET mechanism could be operative in this case. The experimental results of Nishinaga et al.[41] are indeed consistent with the autoxidation mechanism initiated by the one ET.

3. Oxygenation of Flavin Derivatives. The free energies (ΔG) for NADH and flavin derivatives are positive in sign, as shown in Table 9.[45] The CT mechanism could be applicable to these biologically important substances in an aprotic solvent. The ΔG values in aqueous solutions were obtained by substracting 0.24 eV from the values given in Table 9. These values remain slightly positive in sign. Both the CT and one-ET mechanism are conceivable in this case. Therefore, the flavin radical and superoxide (or hydroperoxyl radical) could be formed as discrete intermediates, depending on the environmental effects, such as the pH and temperature. The trends derived from the theoretical calculations are parallel to those of the detailed kinetics concerning the flavin derivatives by Bruice et al.[46]

For example, Bruice and his collaborators have extensively studied the electron-transfer reactions between 1,10-ethano-5-ethyl-1,5-dihydrolumiflavin (**XXIV**) and triplet molecular oxygen. They found that, although the overall oxidation involves the transfer of two electrons, the transition states for $^3O_2$ oxidation of **XXIV** to **XXVII** plus H_2O_2 closely resemble or are identical with the structure of the ion

Table 8. Free Energies (ΔG) for Electron Transfer from 4-Substituted 2,6-Di-*t*-butylphenols (**I**) and 4-Substituted 2,6-Di-*t*-butylanilines (**XXI**) to Triple Molecular Oxygen

Substituents	**I**		**XXI**	
	E_{OX}	ΔG	E_{OX}	ΔG
a (4-Ph)	−0.34	0.46	−1.04	−0.24
b (4-Me)	−0.33	0.47	−1.03	−0.23
c (4-CH_2Ph)	−0.24	0.56	−0.94	−0.14
d (4-t-butyl)	−0.20	0.60	−0.90	−0.10
e (4-CH_2OH)	−0.18	0.62	−0.88	−0.08
f (4-Br)	−0.14	0.66	−0.84	−0.04
g (4-H)	−0.05	0.76	−0.76	0.05
h (4-CO_2Et)	0.15	0.95	−0.55	0.25
Catechol (**XXII**) anion	−0.13	0.67		
XXII dianion	−1.27	−0.47		
XXIII anion[a]	−0.49	0.31		

a) **XXIII**=α-tocopherol.

Table 9. Free Energies (ΔG) for Electron Transfer from NADH and Flavin to $^3O_2$

System			E_{OX}	ΔG
NADH/NAD·	+e	$+H^+$	0.06	0.86 (0.62)
FH_2/FH·	+e	$+H^+$	−0.433	0.37 (0.12)
FH^-/FH·	+e		−0.390	0.41 (0.16)
FH_2^-/FH·	+e	$+H^+$	−0.314	0.49 (0.24)
Ribboflavin			−0.452	0.35 (0.11)
Lumiflavin			−0.477	0.32 (0.07)

radical pair [**XXV** $O_2^{-\cdot}$], which is formed by endothermic charge transfer from **XXIV** to triplet molecular oxygen. A covalent intermediate, which could be the 4a-peroxidoflavin zwitterion (ZW), is formed upon the collapse of the transition state. The ZW intermediate hydrolyzes to H_2O_2 and the two-electron oxidized flavin in aqueous solution, while it provides the hydroperoxide in nonaqueous solution. Thus the CTSI mechanisms could be operative for the endothermic oxygenations of flavins, as described by Scheme 4.

On the other hand, Bruce has shown that the superoxide and flavin radical result as discrete intermediates if the flavin analogs have electron-donating substituents. Thus, it is in harmony with the fact that the free energies for the one-electron transfers of flavin derivatives to triplet molecular oxygen are nearly zero in an aqueous solution, as shown in Table 9. The spin inversion is not necessary for the oxygenation passing through the complete one-ET mechanism, as has been emphasized by Bruice.[46]

Conclusion

The present theoretical results indicate that the ET BR characters in CT complexes (**3**) are sensitive to environmental effects, such as the solvents and counter ions, since the substrate-oxygen bonding in **3** are labile. Theoretical studies further suggest that the singlet and triplet CT states couple with each other through a spin–orbit interaction, breaking the so-called spin conservation rule. This is attributable to the small energy gap between the states and the orthogonality for the radical orbitals. These results in turn imply that the controls of the electronic and spin properties of **3** by solvents and metal ions could be particularly important for the clean and selective oxygenations of substrates (**I-XXV**) examined here, since the oxygenations often suffer contamination arising from autoxidations induced by the one ET (**2**). However, further refinements and extensions of the relationships in Figs. 10 and 11 are necessary for a theoretical approach toward the goal.

The electronic states of the ternary complexes comprising molecular oxygen, substrate anions and gegen ions are variable from the closed-shell ions (**1**) to one ET biradical (**2**) through the intermediate CT complexes (**3**), as shown in Eq. 1. From our MO-theoretical view point, these variations

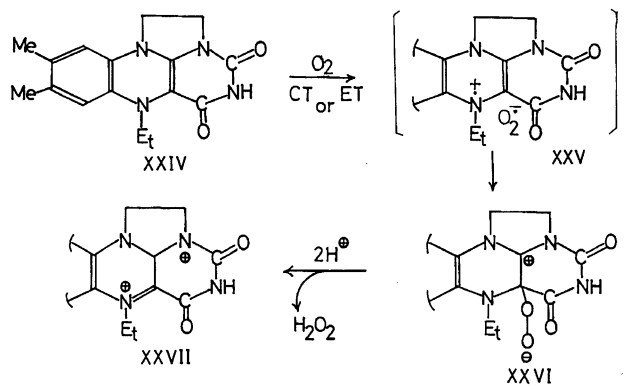

Scheme 4.

are parallel to those of the tricentric bisdesmiphiles and 1, 4-peroxy dipoles examined previously.[24e,24f] This in turn indicates that ab initio post Hartree–Fock calculations will be necessary in the future to confirm the potential curves drawn by the semiempirical techniques. Particularly, CASSCF calculations involving the spin–orbit interaction are essential for elucidating the spin-inversion process within the CT complexes in Fig. 7B.

The charge-transfer followed by the spin-inversion (CTSI) model presented here could be applied to the selective transition-metal promoted oxygenation of phenol, catechol and indole derivatives and their biological oxygenations catalyzed by dioxygenases. We obtained the following conclusions for these species from the numerical results given in Tables 5 and 6:

(1) The reactions of the carbanion and triplet molecular oxygen proceed through a one-ET mechanism from carbanion to $^3O_2$ in aprotic and protic solvents, showing that the radical chain mechanism is operative in the oxygenation reactions of these species, in accord with the Russel mechanism.[20]

(2) In phenol and its derivatives, the base-promoted phenol monoanion reacts with molecular oxygen via two different mechanisms. One is the CT mechanism, where a triplet charge-transfer (CT) complex is formed and a spin inversion from the ^{3}CT complex to the ^{1}CT complex occurs in aprotic solvents. The other is a one-electron transfer mechanism assisted by strong hydrogen bonding in a protic solvent.

(3) In the indole and its derivatives, a complete electron transfer does not occur, even if the O–O bond distance is extremely elongated, indicating that free monoanions of indole derivatives are not very sensitive to triplet molecular oxygen. These species are, however, readily oxygenated by organo-metal catalysts, such as organo-cobalt, followed by the formation of a hydroxocobalt complex. The CTSI mechanism is reasonable in the case of the metal-catalyzed oxygenation reactions of indole derivatives by Nishinaga et al.[17–19]

(4) For the flavin derivatives, the CT mechanism is applicable in an aprotic solution, while both the CT and one-ET mechanisms are conceivable in an aqueous solution. The flavin radical and superoxide (or hydroperoxyl radical) are formed as discrete intermediates in an aqueous solution. This is compatible with the conclusions by Bruice et al.[46]

References

1) "Oxygenases," ed by O. Hayaishi, Academic Press, New York (1962).

2) G. A. Hamilton, "Molecular Mechanism of Dioxygen Activation," ed by O. Hayaishi, Academic Press, New York (1974), p. 405.

3) T. Matsuura, *Tetrahedron*, **33**, 2869 (1977).

4) R. A. Sheldon and J. K. Kochi, "Metal-Catalyzed Oxidations of Organic Compounds," Academic Press, New York (1981).

5) L. I. Simandi, "Catalytic Activation of Dioxygen by Metal Complexes," Kluwer, Amsterdam (1992).

6) D. T. Sawyer, "Oxygen Chemistry," Oxford University

Press, Oxford (1991).

7) "Oxygen Complexes and Oxygen Activation by Transition Metals," ed by A. E. Martell and D. T. Swayer, Plenum, New York (1987).

8) "Organic Peroxides," ed by D. Swern, Wiley Interscience, New York (1971).

9) M. Nozaki, *Top. Curr. Chem.*, **78**, 145 (1978).

10) a) R. D. Jones, D. A. Summerville, and F. Basolo, *Chem. Rev.*, **79**, 139 (1979); b) E. C. Niederhoffer, J. H. Timmons, and A. E. Martell, *Chem. Rev.*, **84**, 137 (1984).

11) a) L. Que, Jr., J. D. Lipscomb, R. Zimmermann, E. Münck, N. R. Orme-Johnson, and W. H. Orme-Johnson, *Biochem. Biophys. Acta*, **452**, 320 (1976); b) L. Que, Jr., J. D. Lipscomb, E. Münck, and J. M. Wood, *Biochem. Biophys. Acta*, **485**, 60 (1977).

12) Y. Tatsuno, Y. Saeki, M. Iwaki, T. Yagi, M. Nozaki, T. Kitagawa, and S. Otsuka, *J. Am. Chem. Soc.*, **100**, 4614 (1978).

13) a) T. Funabiki, A. Mizoguchi, T. Sugimoto, S. Tada, M. Tsuji, H. Sakamoto, and S. Yoshida, *J. Am. Chem. Soc.*, **108**, 2921 (1986); b) T. Funabiki, T. Konishi, S. Taka, and S. Yoshida, *Chem. Lett.*, **1987**, 1803; c) T. Funabiki, H. Kojima, M. Kaneko, T. Inoue, T. Yoshioka, T. Tanaka, and S. Yoshida, *Chem. Lett.*, **1991**, 2143; d) T. Funabiki, I. Yoneda, M. Ishikawa, M. Ujiie, Y. Nagai, and S. Yoshida, *J. Chem. Soc., Chem. Commun.*, **1994**, 453.

14) a) L. Que, Jr., R. C. Kolanczyk, and L. S. White, *J. Am. Chem. Soc.*, **109**, 5373 (1987); b) U. G. Jang, D. D. Cox, and L. Que, Jr., *J. Am. Chem. Soc.*, **113**, 9200 (1991).

15) S. Fujii, H. Ohya-Nishiguchi, N. Hirota, and A. Nishinaga, *Bull. Chem. Soc. Jpn.*, **66**, 1408 (1993).

16) a) L. Que, Jr., J. Widom, and R. L. Crawford, *J. Biol. Chem.*, **256**, 10941 (1981); b) R. H. Heistrand, II, R. B. Lauffer, E. Fikrig, and L. Que, Jr., *J. Am. Chem. Soc.*, **104**, 2789 (1982); c) J. M. Wood, "Metal Ions Activations of Dioxygen," ed by T. G. Spiro, John Wieley & Sons, Inc., New York (1980), Chap. 4.

17) a) A. Nishinaga, M. Yano, T. Kuwashige, K. Maruyama, and T. Mashino, *Chem. Lett.*, **1994**, 817; b) A. Nishinaga, H. Iwasaki, T. Shimizu, Y. Toyoda, and T. Matsuura, *J. Org. Chem.*, **51**, 2257 (1986); c) A. Nishinaga, H. Iwasaki, T. Kondo, and T. Matsuura, *Chem. Lett.*, **1985**, 5; d) A. Nishinaga, T. Shimizu, Y. Toyoda, T. Matsuura, and K. Hirotsu, *J. Org. Chem.*, **47**, 2278 (1982); e) A. Nishinaga, H. Tomita, K. Nishizawa, T. Matsuura, S. Ooi, and K. Hirotsu, *J. Chem. Soc., Dalton Trans.*, **1981**, 1504; f) A. Nishinaga, T. Shimizu, T. Fujii, and T. Matsuura, *J. Org. Chem.*, **45**, 4997 (1980); g) A. Nishinaga, T. Shimizu, and T. Matsuura, *Tetrahedron Lett.*, **1978**, 3747; *J. Org. Chem.*, **44**, 2983 (1979); h) A. Nishinaga, T. Itahara, T. Shimizu, and T. Matsuura, *J. Am. Chem. Soc.*, **100**, 1820 (1978); i) A. Nishinaga, T. Itahara, T. Matsuura, A. Rieker, D. Koch, K. Albert, and P. B. Hitchcock, *J. Am. Chem. Soc.*, **100**, 1826 (1978); j) A. Nishinaga, T. Shimizu, and T. Matsuura, *Tetrahedron Lett.*, **1978**, 3747; k) A. Nishinaga, T. Itahara, T. Shimizu, H. Tomita, K. Nishizawa, and T. Matsuura, *Photochem. Photobiol.*, **28**, 687 (1978); l) A. Nishinaga, T. Shimizu, and T. Matsuura, *Chem. Lett.*, **1977**, 547; m) A. Nishinaga, T. Itahara, and T. Matsuura, *Chem. Lett.*, **1974**, 667.

18) a) A. Nishinaga, T. Tsutsui, H. Moriyama, T. Wazaki, T. Mashino, and Y. Fujii, *J. Mol. Catal.*, **83**, 117 (1993); b) A. Nishinaga, H. Ohara, H. Tomita, and T. Matsuura, *Tetrahedron Lett.*, **24**, 213 (1983).

19) a) A. Nishinaga, T. Kuwashige, T. Tsutsui, T. Mashino, and K. Maruyama, *J. Chem. Soc., Dalton Trans.*, **1994**, 805; b) W. Hiller, A. Nishinaga, and A. Rieker, *Z. Naturforsch., B*, **47b**, 1185 (1992); c) A. Nishinaga, N. Numada, and K. Maruyama, *Tetrahedron Lett.*, **30**, 2257 (1989); d) A. Nishinaga, T. Tojo, H. Tomita, and T. Matsuura, *J. Chem. Soc., Perkin Trans. 1*, **1979**, 2511.

20) a) G. A. Russel, E. G. Janzen, A. G. Bemis, E. J. Geels, A. J. Moye, S. Mak, and E. T. Strom, *Adv. Chem. Ser.*, **51**, 111 (1965); b) G. A. Russell, A. G. Bemis, E. J. Geels, E. G. Janzen, and A. J. Moye, *Adv. Chem. Ser.*, **75**, 174 (1968).

21) a) C. Walling and S. A. Buchler, *J. Am. Soc.*, **77**, 6032 (1955); b) C. Walling and S. A. Buchler, *Adv. Chem. Ser.*, **75**, 166 (1968).

22) a) K. Yamaguchi, *Jpn. Chem. Rev.*, **1**, 294 (1973), and Thesis, Osaka University, 1972; b) K. Yamaguchi, Y. Ikeda, and T. Fueno, "The 16th Oxygenation Symposium," Kyoto, 1983, and *Tetrahedron*, **41**, 2099 (1985); c) K. Yamaguchi, "Singlet Oxygen," ed by A. A. Frimer, CRC Press, Boca Raton (1985), Vol. III, Chap. 2.

23) a) N. J. Turro, V. Ramamurthy, K. -C. Liu, A. Krebs, and R. Kemper, *J. Am. Chem. Soc.*, **98**, 6758 (1976); b) N. J. Turro, Y. Ito, and M. -F. Chow, *J. Am. Chem. Soc.*, **99**, 5836 (1977).

24) a) T. Takabe and K. Yamaguchi, *Chem. Phys. Lett.*, **40**, 347 (1976); b) T. Takabe, K. Takenaka, K. Yamaguchi, and T. Fueno, *Chem. Phys. Lett.*, **44**, 65 (1976); c) K. Yamaguchi and T. Fueno, *Chem. Phys.*, **19**, 35 (1977); d) K. Yamaguchi and T. Fueno, *Chem. Phys.*, **23**, 375 (1977); e) Y. Yoshioka, D. Yamaki, G. Murata, M. Nishino, T. Tsunesada, and K. Yamaguchi, *Bull. Chem. Soc. Jpn.*, submitted; f) Y. Yoshioka, D. Yamaki, G. Murata, M. Nishino, K. Yamaguchi, and K. Mizuno, *Bull. Chem. Soc. Jpn.*, submitted.

25) a) J. Wilshire and K. T. Sawyer, *Acc. Chem. Res.*, **12**, 105 (1979); b) D. T. Sawyer and J. S. Valentine, *Acc. Chem. Res.*, **14**, 393 (1981).

26) J. L. Pack and A. V. Phelps, *J. Chem. Phys.*, **44**, 1870 (1966).

27) W. T. Zemke, G. Das, and A. C. Wahl, *Chem. Phys. Lett.*, **14**, 310 (1972).

28) M. Arshadi and P. Kebarle, *J. Phys. Chem.*, **74**, 1483 (1970).

29) A. U. Kahn, *Photochem. Photobiol.*, **28**, 615 (1978).

30) P. A. Narayam, D. Suryanarayama, and L. Kevan, *J. Am. Chem. Soc.*, **104**, 3552 (1982).

31) J. Eriksen and C. S. Foote, *J. Phys. Chem.*, **82**, 2659 (1978).

32) a) H. Tatewaki and H. Hujinaga, *J. Chem. Phys.*, **72**, 4339 (1980), and their series of papers; b) P. J. Hay, *J. Chem. Phys.*, **66**, 4377 (1977).

33) a) A. Dedieu and M. M. Rohmer, *J. Am. Chem. Soc.*, **99**, 8050 (1977); b) B. D. Olafson and W. A. Goddard, III, *Proc. Natl. Acad. Sci. U.S.A.*, **74**, 1315 (1977); c) R. F. Kirchner and G. H. Loew, *J. Am. Chem. Soc.*, **99**, 4639 (1977); d) D. A. Case, B. H. Huynh, and M. Karplus, *J. Am. Chem. Soc.*, **101**, 4433 (1979); e) A. Dedieu, M. M. Rohmer, H. Veillard, and A. Veillard, *Nouv. J. Chem.*, **3**, 653 (1979); f) Z. S. Herman and G. H. Loew, *J. Am. Chem. Soc.*, **102**, 1815 (1980); g) T. Nozawa, M. Hatano, U. Nagashima, S. Obara, and H. Kashiwagi, *Bull. Chem. Soc. Jpn.*, **56**, 1721 (1983).

34) a) E. A. Mayeda and A. J. Bard, *J. Am. Chem. Soc.*, **95**, 6223 (1973); **96**, 4023 (1974); b) W. H. Koppennol and J. Butler, *FEBS Lett.*, **83**, 1 (1977); c) C. S. Foote, F. C. Shook, and R. A. Abakerli, *J. Am. Chem. Soc.*, **102**, 2503 (1980).

35) a) A. U. Khan and M. Kasha, *J. Am. Chem. Soc.*, **92**, 3293 (1970); b) W. C. Danen and R. L. Arudi, *J. Am. Chem. Soc.*, **100**, 3944 (1978); c) W. Adam, O. Cueto, and H. Rebollo, *Angew. Chem.*, **94**, 82 (1982).

36) Y. Yoshioka, T. Kawakami, S. Yamada, M. Nishino, K. Yamaguchi, and I. Saito, *Bull. Chem. Soc. Jpn.*, **69**, 2683 (1996).

37) L. N. Domelsmith, L. L. Munchausen, and K. N. Houk, *J. Am. Chem. Soc.*, **99**, 4311 (1977).

38) A. A. Gorman, G. Lovering, and M. A. J. Rogers, *J. Am.*

Chem. Soc., **101**, 3050 (1979).
39) M. J. Thomas and C. S. Foote, *Photochem. Photobiol.*, **27**, 683 (1978).
40) D. Rehm and A. Weller, *Ber. Bunsenges. Phys. Chem.*, **73**, 834 (1969).
41) A. Nishinaga, T. Itahara, K. Nakamura, T. Matsuura, A. Rieker, J. Bracht, and H. J. Lindner, *Tetrahedron*, **34**, 3037 (1978).
42) a) Y. Morooka and C. S. Foote, *J. Am. Chem. Soc.*, **98**, 1510 (1976); b) Sawaki and C. S. Foote, *J. Am. Chem. Soc.*, **101**, 6292 (1979).
43) Y. Saeki, M. Nozaki, and S. Seroh, *J. Biol. Chem.*, **255**, 8465 (1980).
44) W. von E. Doering and R. M. Haines, *J. Am. Chem. Soc.*, **76**, 482 (1954).
45) R. F. Williams, S. Shikai, and T. C. Bruice, *Proc. Natl. Acad. Sci. U.S.A.*, **72**, 1763 (1975).
46) a) C. Kemal, T. W. Chan, and T. C. Bruice, *J. Am. Chem. Soc.*, **99**, 7272 (1977); b) G. Eberlein and T. C. Bruice, *J. Am. Chem. Soc.*, **104**, 1449 (1982); **105**, 6685 (1983).